3d IMS Turbulence Workshop *Informal discussions on fractal-generated turbulence*
Institute for Mathematical Sciences, Imperial College London , 18 and 19 February 2008

FIRST EXPERIMENTS AT ICL ON FRACTAL GRID TURBULENCE USING MULTI-HOT-WIRE TECHNIQUES

Michael Kholmyansky[1] and Arkady Tsinober[1,2]
[1]Tel Aviv Israel, [2]ICL, UK

The emphasis here is on qualitative aspects.

The experiments were performed at summer 2006 by the team of three: G.Gulitskii, M. Kholmyansky and S. Yorish.

The emphasis here is on qualitative aspects.

This is a first set of experiments with the main motivation (but not the only) to evaluate the **feasibility** of using the multi-hot-wire system in studies of fractal generated turbulence **with the emphasis on what can be done**. **The outcome is essentially positive**, but it has to be stressed that all results are crude and require checking, especially as concerns the quantitative aspects, e.g. numbers. Therefore the presented results can be seen as preliminary and mostly qualitative only.

All the results below refer to the centerline only.

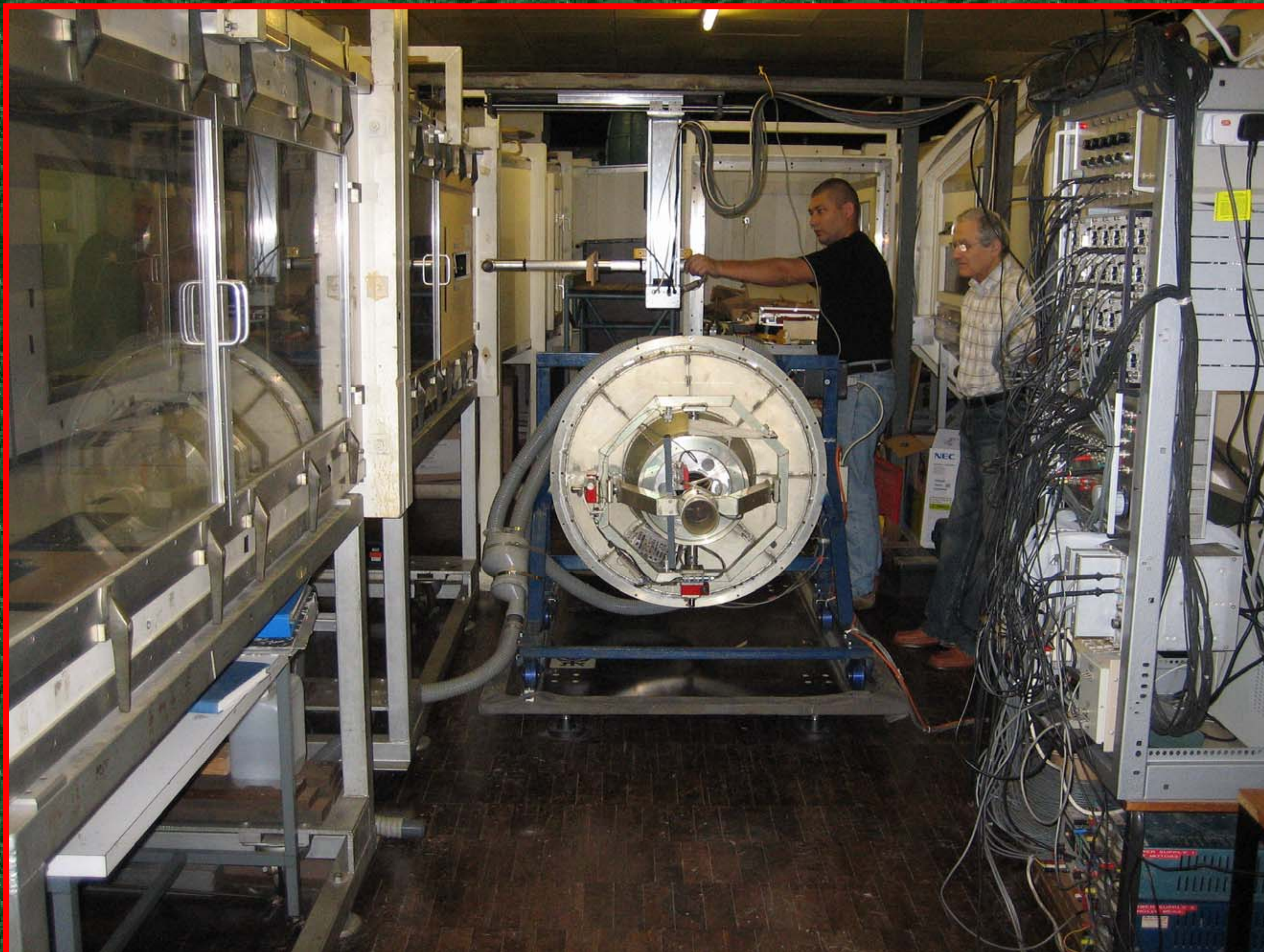
NEC

THE PROBE

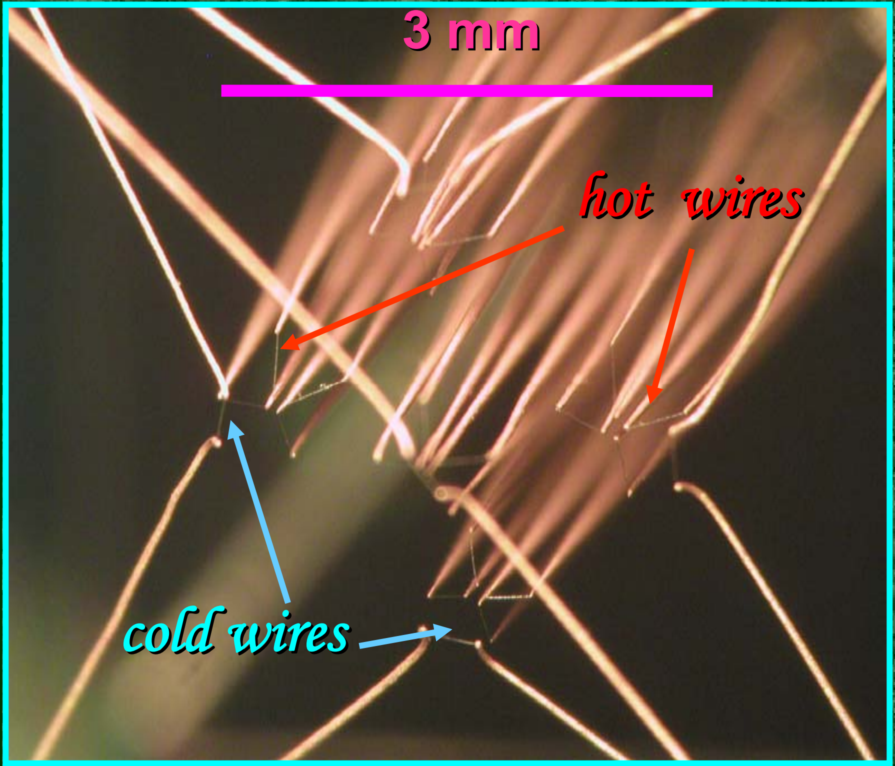

The tip of the probe

Manganin is used as a material for the sensor prongs instead of tungsten because the temperature coefficient of the electrical resistance of manganin is 400 times smaller than that of tungsten.

The calibration unit

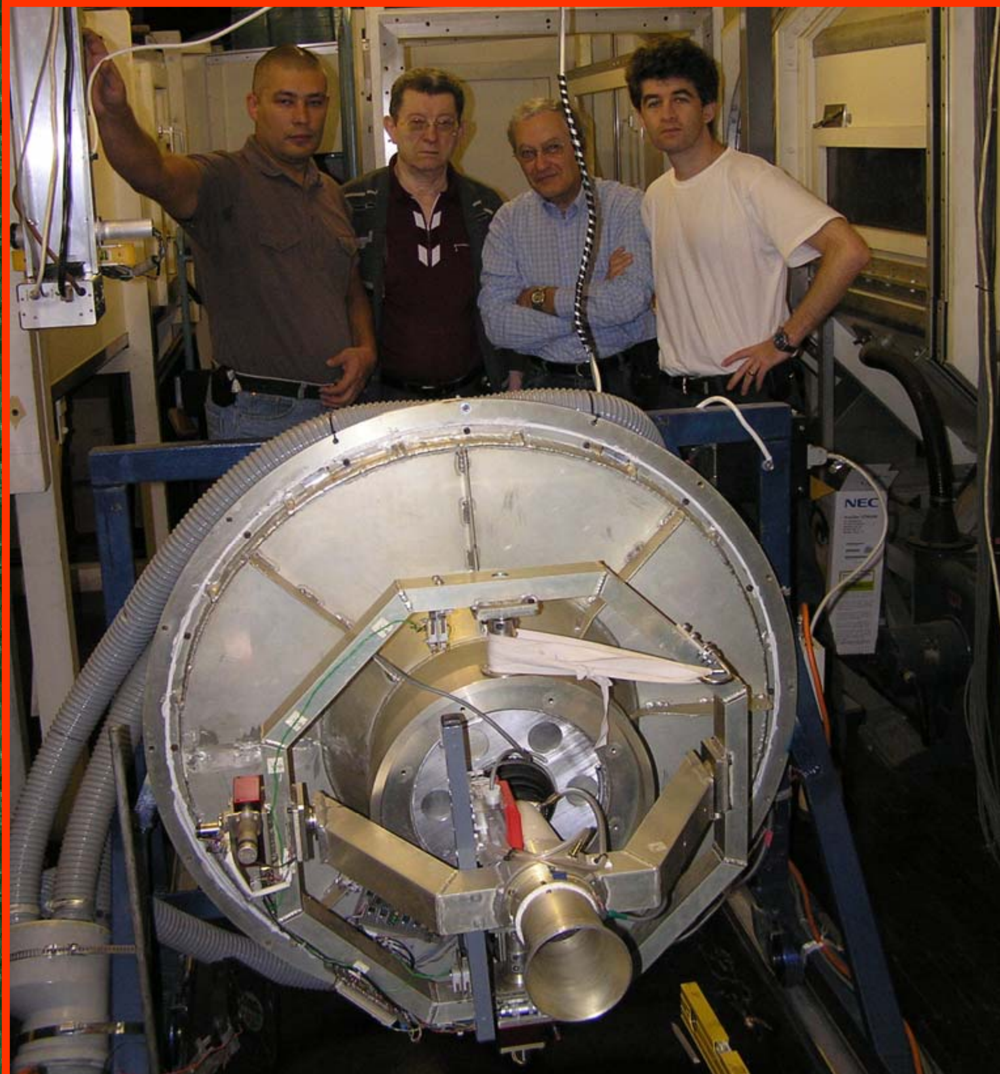

Probe in calibration position

The noise of the system is below 0.15% in RMS

Misha and Probe in calibration position


OLYMPUS
SZX12
OLYMPUS
OLYMPUS

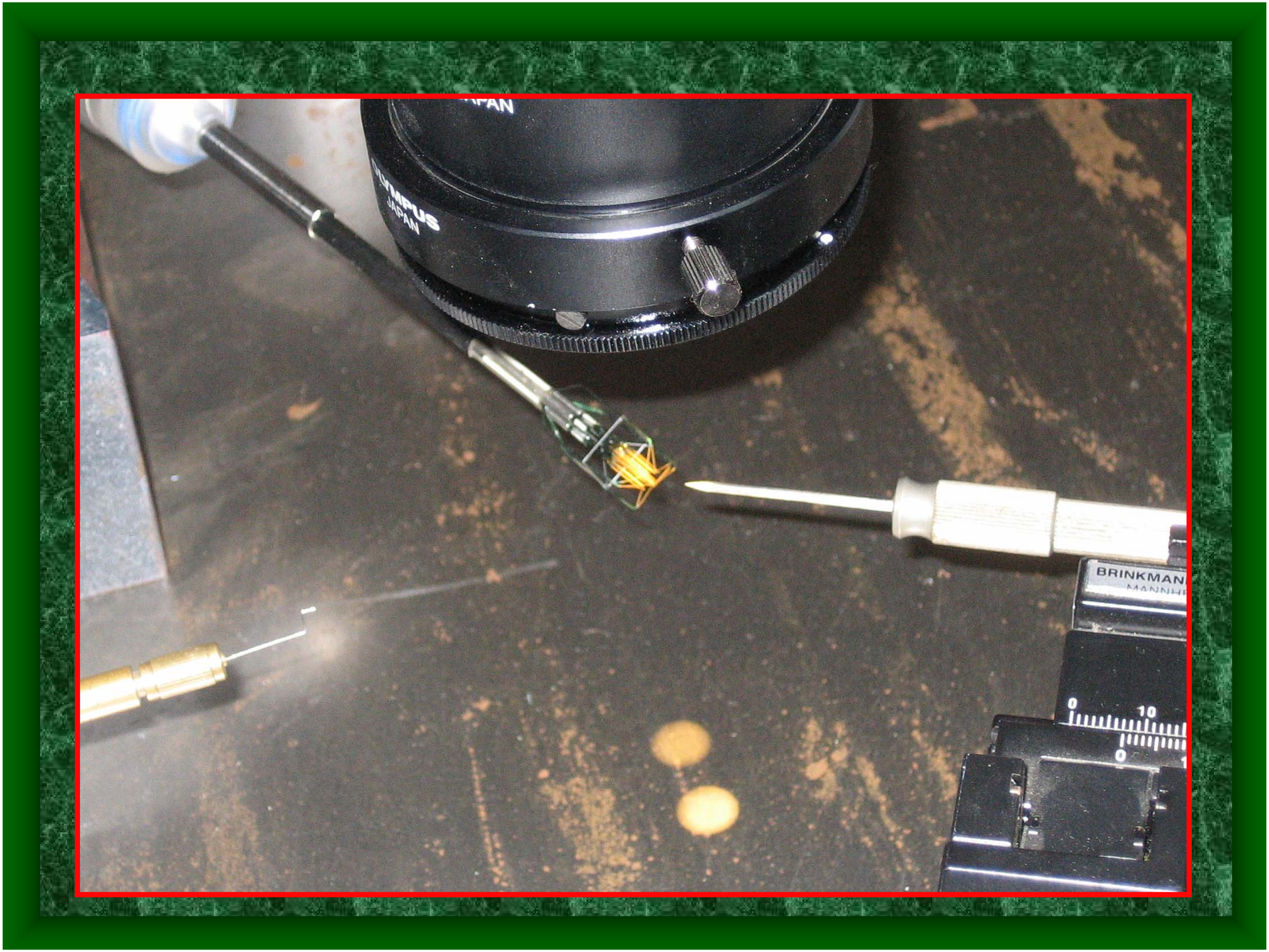
OLYMPUS
JAPAN

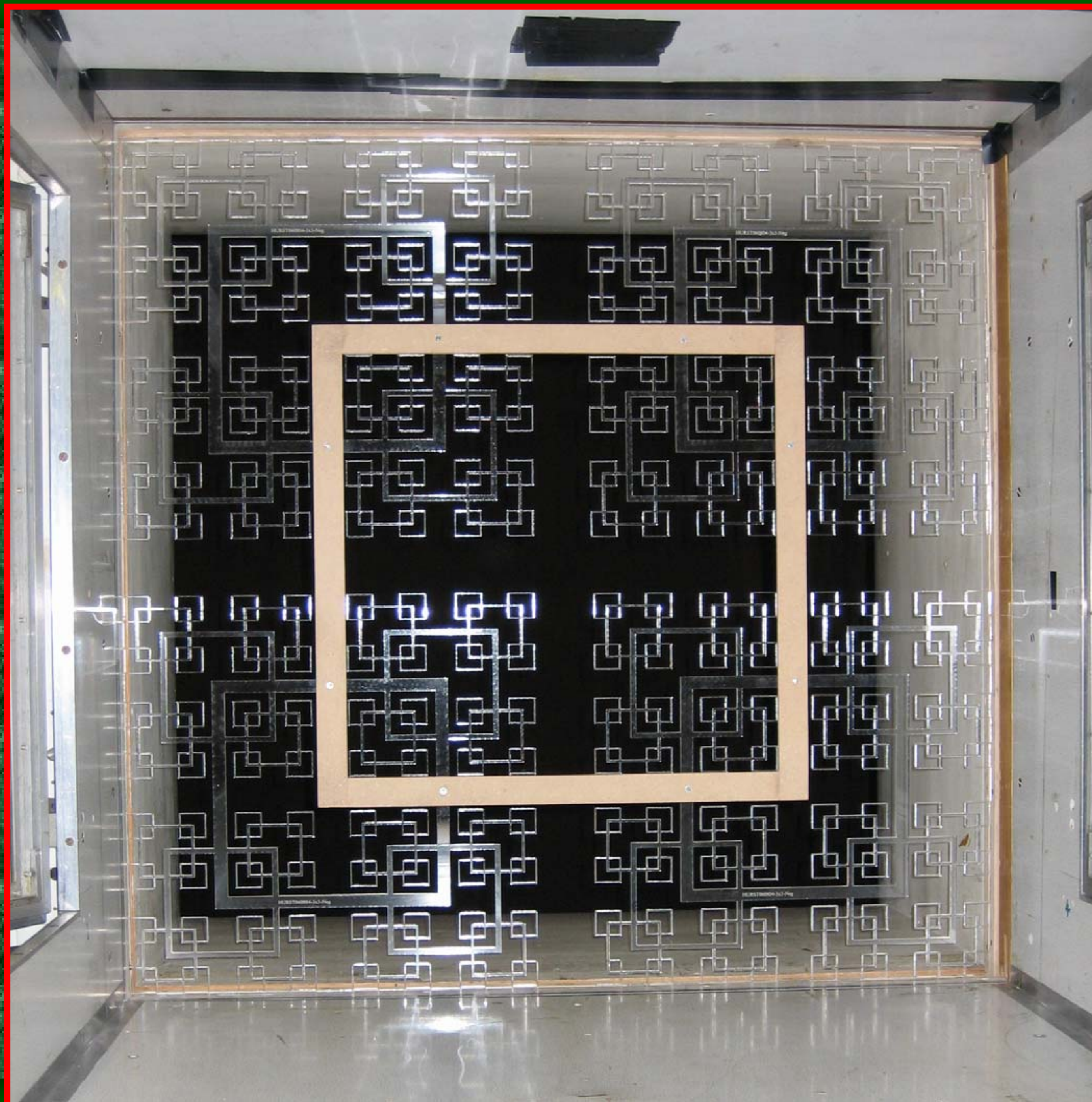

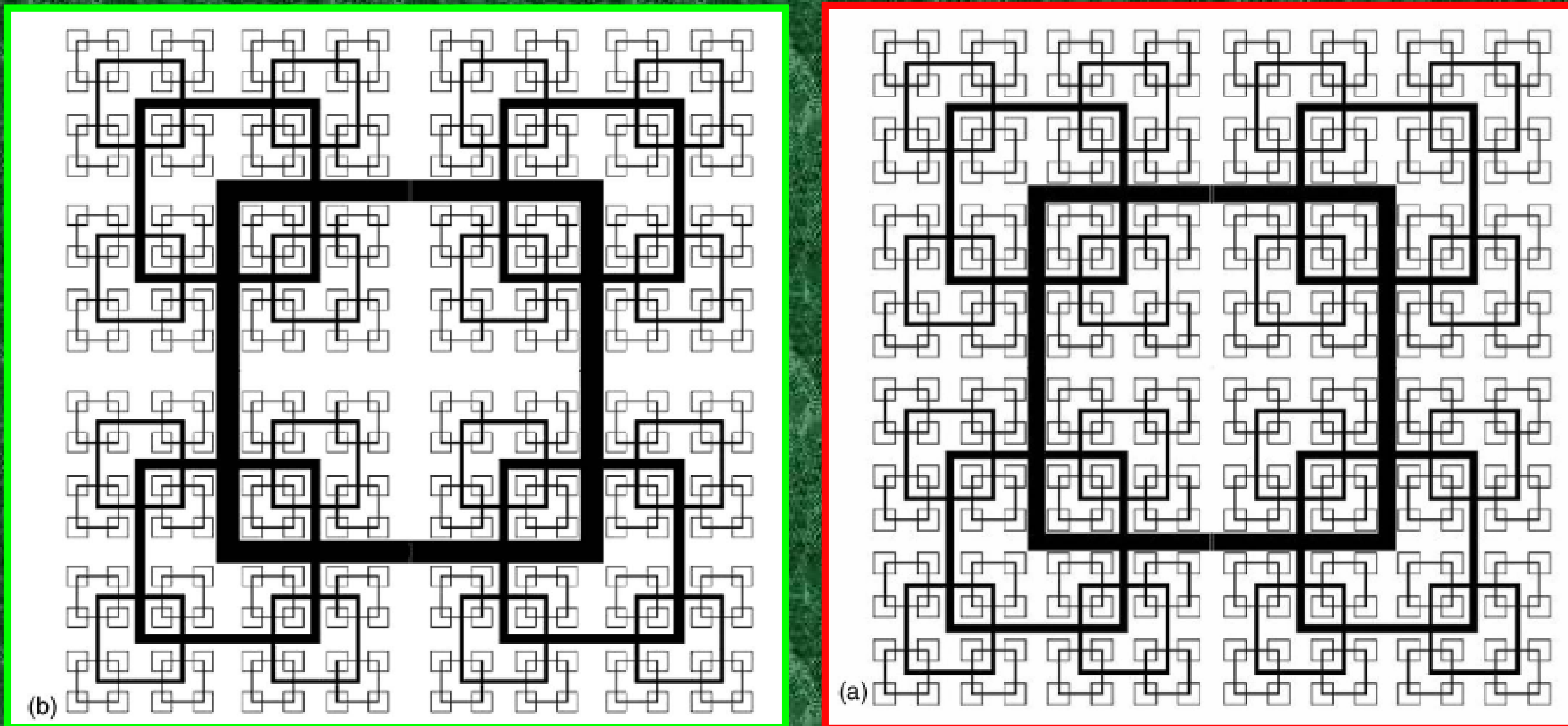

TABLE VII. T=0.91 m tunnel square grid geometry. The errors on σ are estimated by assuming the thickness of each iteration to be accurate within plus/minus the diameter of the manufacturing cutting laser (0.15 mm).

N	D_f	β_t	β_L	σ (%)	M_{eff} (mm)	t_r	R_t
5	2.00	0.00	0.00	25±2.0	26.6	17.0	0.49
5	2.00	−0.18	−0.21	25±1.7	28.6	28.0	0.43


3' x 3' LOW SPEED WIND TUNNEL
40 b.h.p. MOTOR
WIDE ANGLE DIFFUSER
SCREEN K = 2·5
9' x 9' SETTLING CHAMBER
AIR
18' REMOVABLE WORKING (SECTION. (3' x 3' Cross Section)
CONTRACTION Designed by Hodograph method.
3 SCREENS K = 1·6
HONEYCOMB
TOP SPEED ≈ 150 ft sec. TURBULENCE LEVEL ≈ 0·05 %
18' LONG WORKING SECTION WITH REMOVABLE SECTION, AND SHEAR FLOW GRIDS.
FAN CAPABLE OF OPERATION OVER POWER FACTOR RANGE 0·5 – 2

Grid 1- Tr 28

Grid 2- Tr 17

Mean Velocity and Fluctuation RMS

Grid 1- Tr 28 **Grid 2- Tr 17**

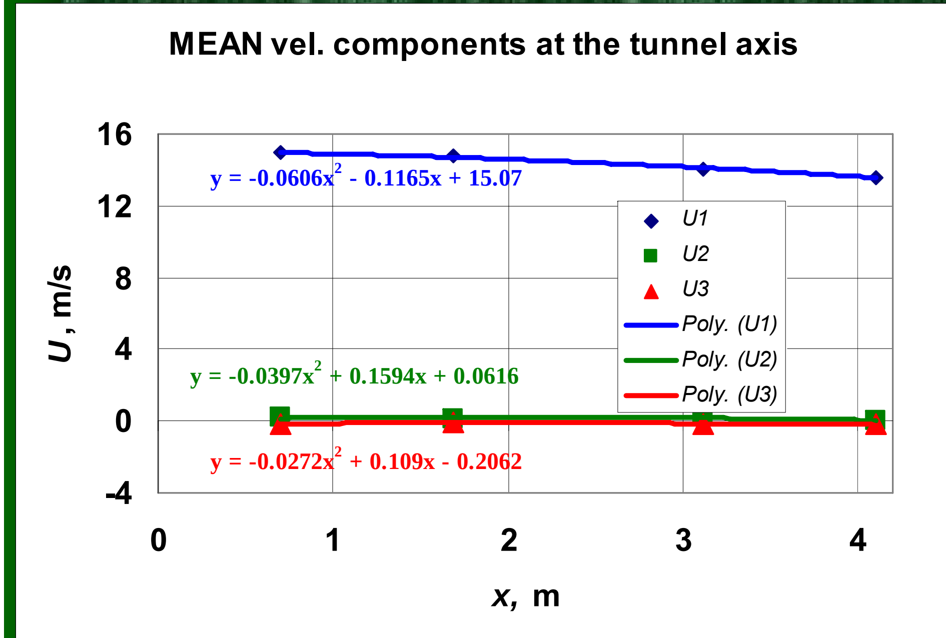

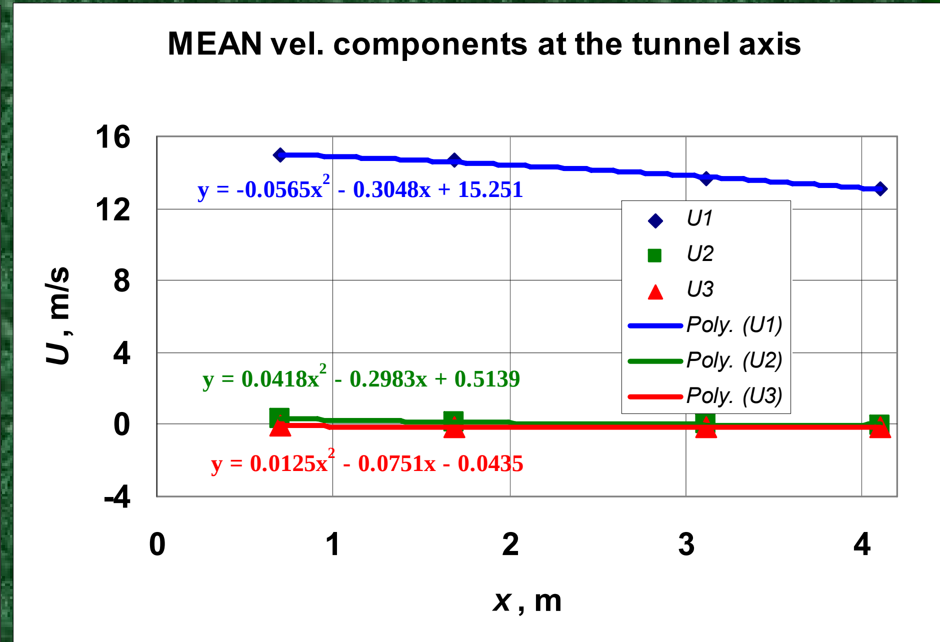

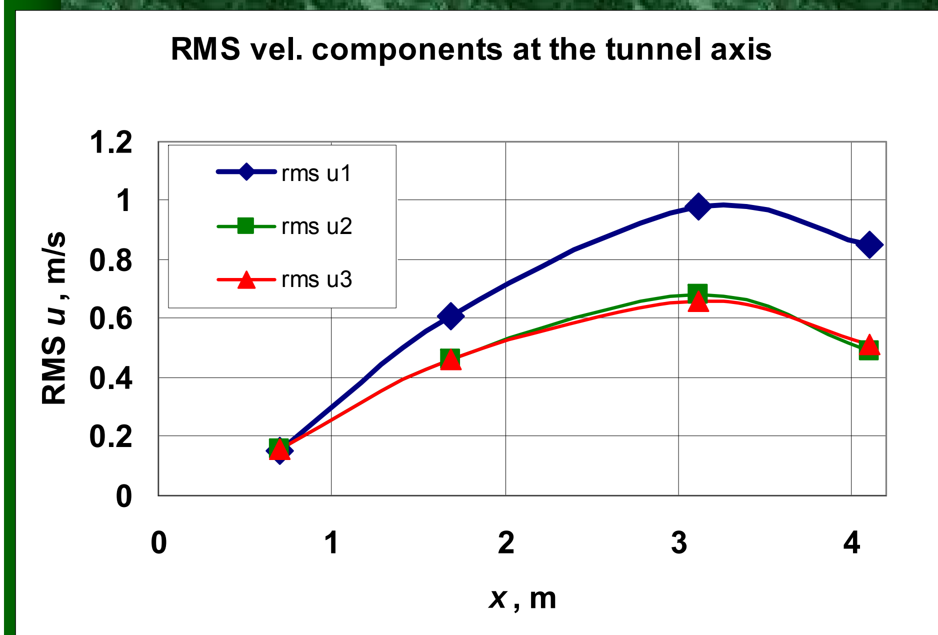

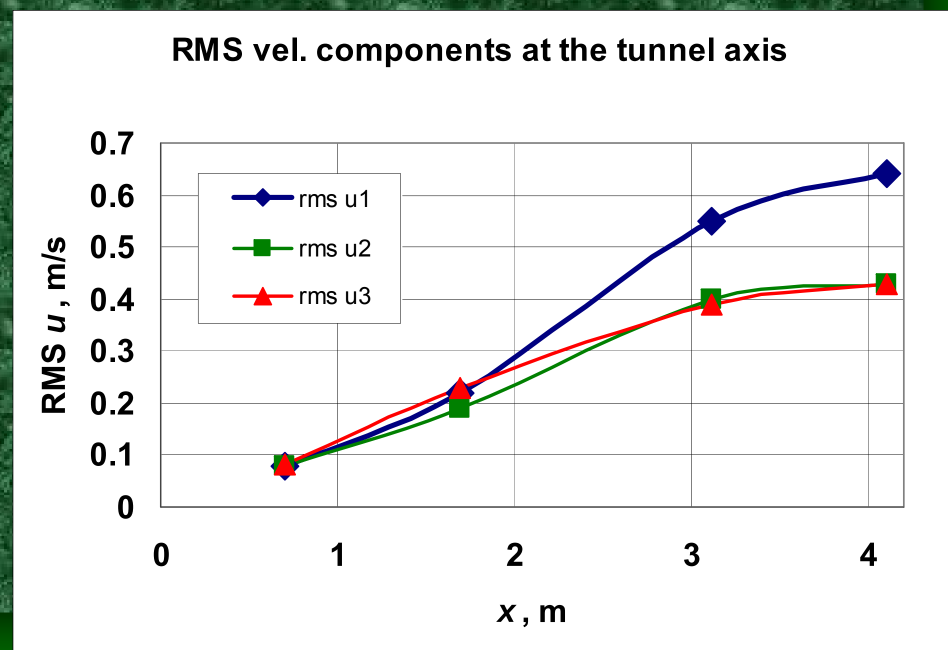

TURBULENT ENERGY PRODUCTION

Grid 1- Tr 28

Grid 2- Tr 17

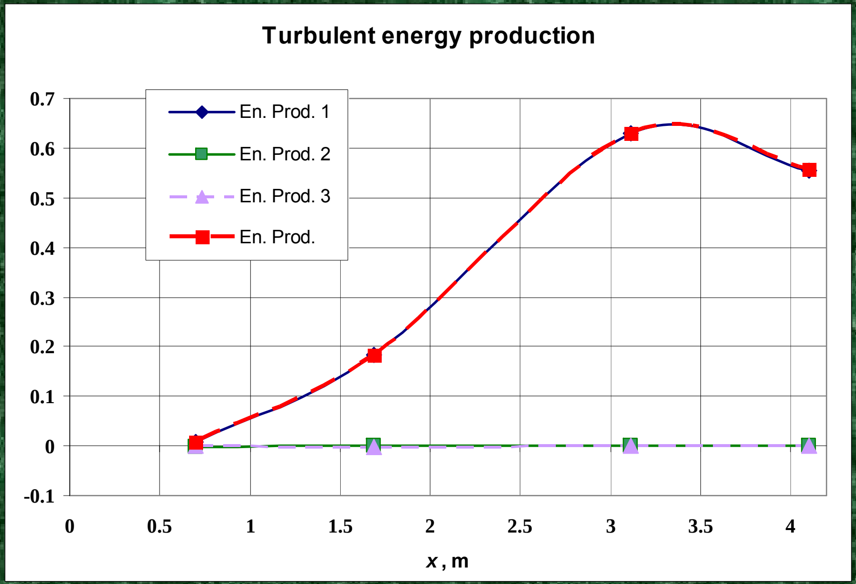

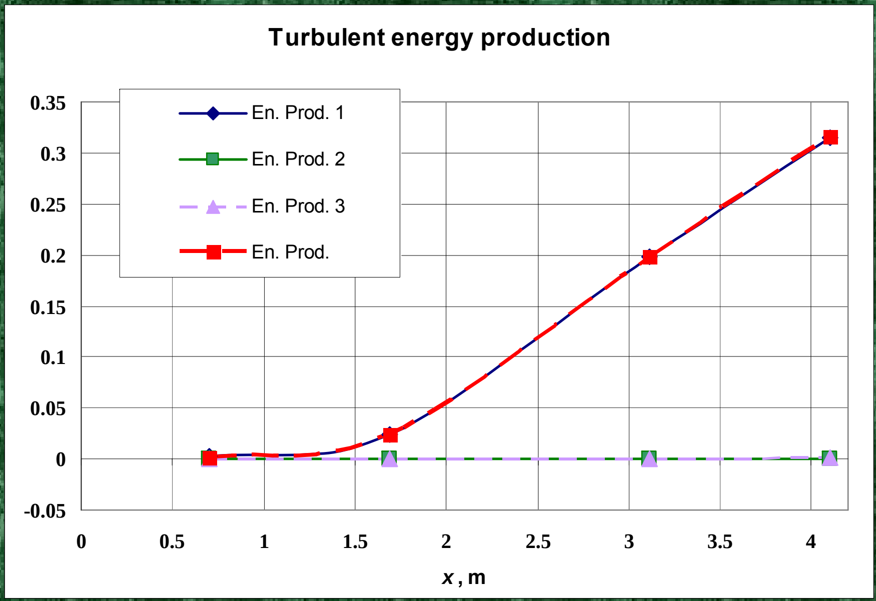

ISOTROPY INDICATORS
velocity

Grid 1- Tr 28

Grid 2- Tr 17

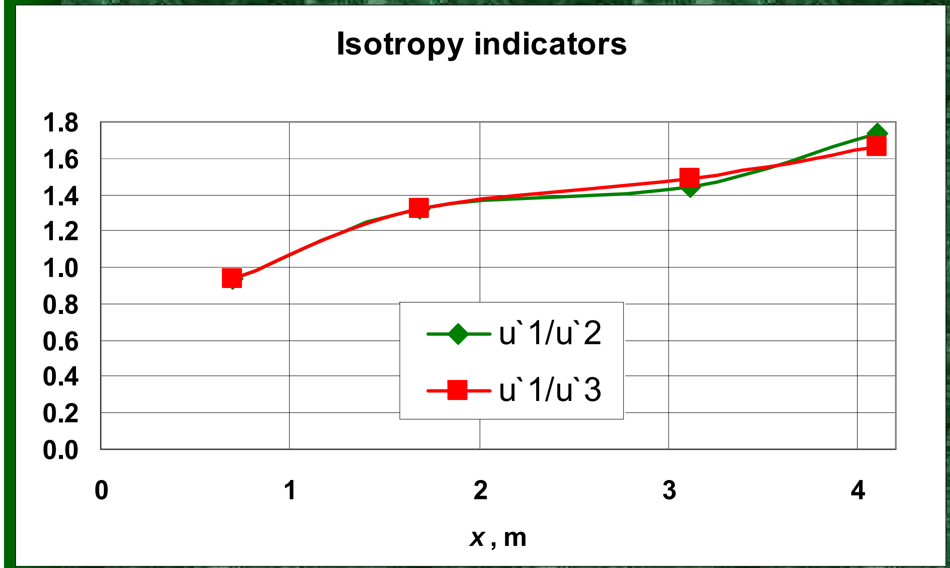

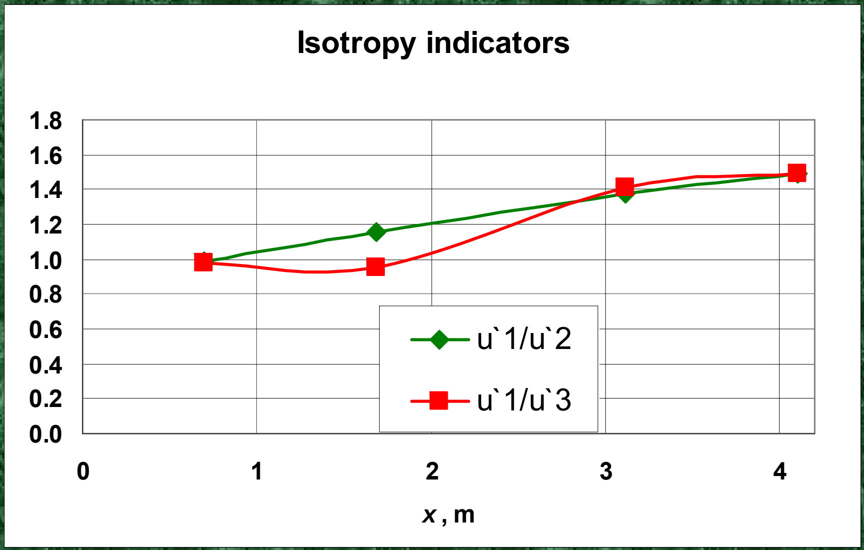

ISOTROPY INDICATORS

velocity derivatives- grid Tr28

1	2	2
2	1	2
2	2	1

$$\partial u_i / \partial x_k$$

X= 3.1m

1.00	1.15	1.05
1.69	1.03	1.21
1.57	1.05	0.74

X= 4.1m

1.00	0.73	0.79
1.60	0.63	0.84
1.62	0.66	0.52

Integral and Taylor Micro-scales

Grid 1- Tr 28

Grid 2- Tr 17

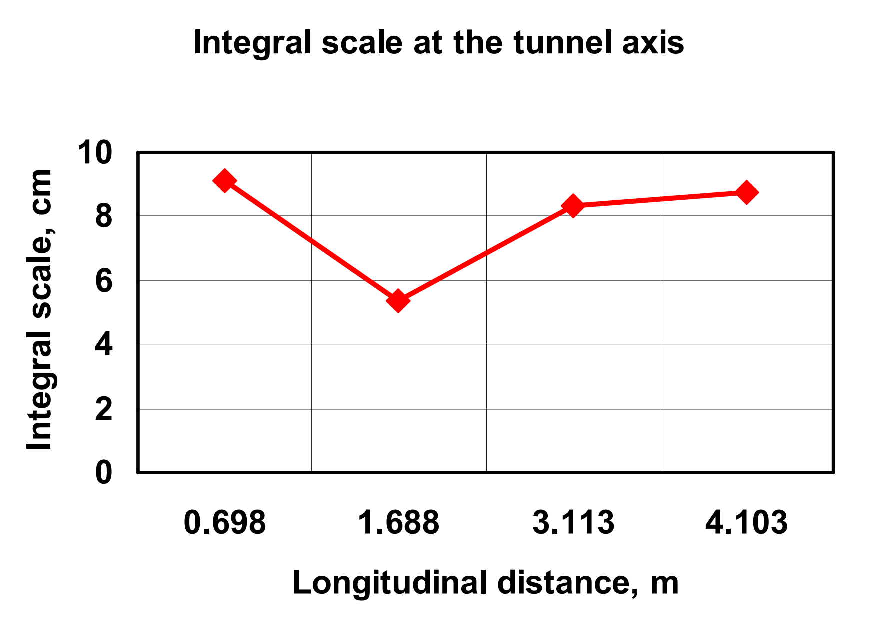

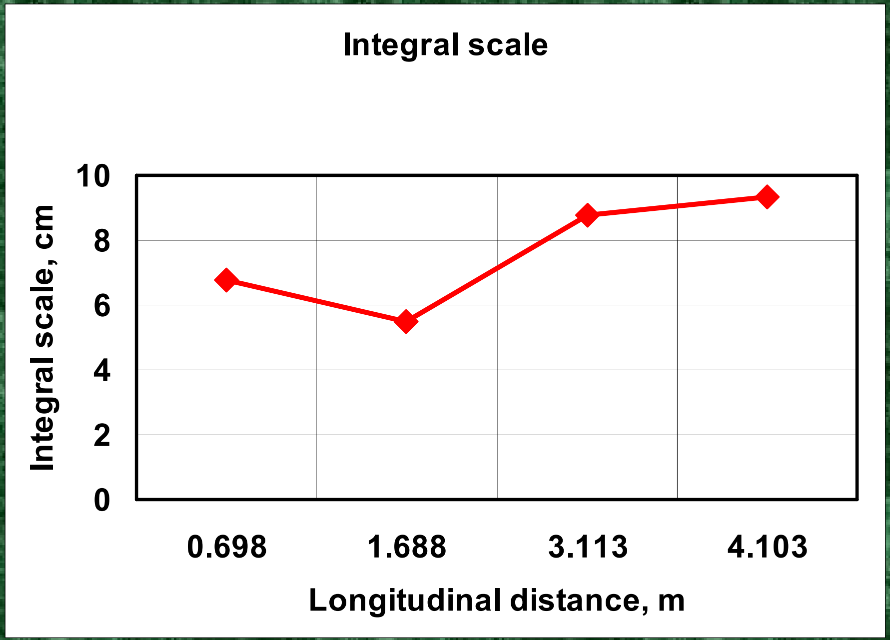

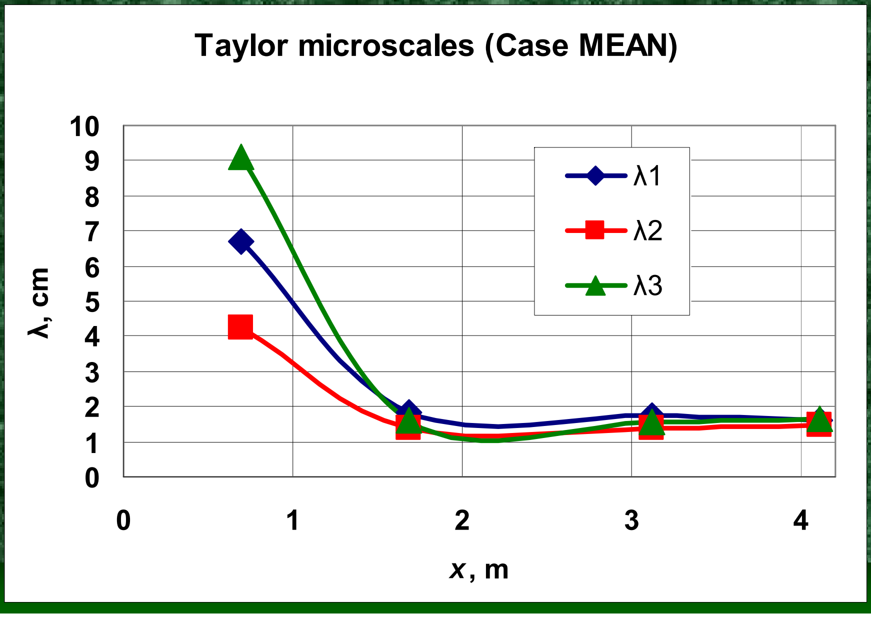

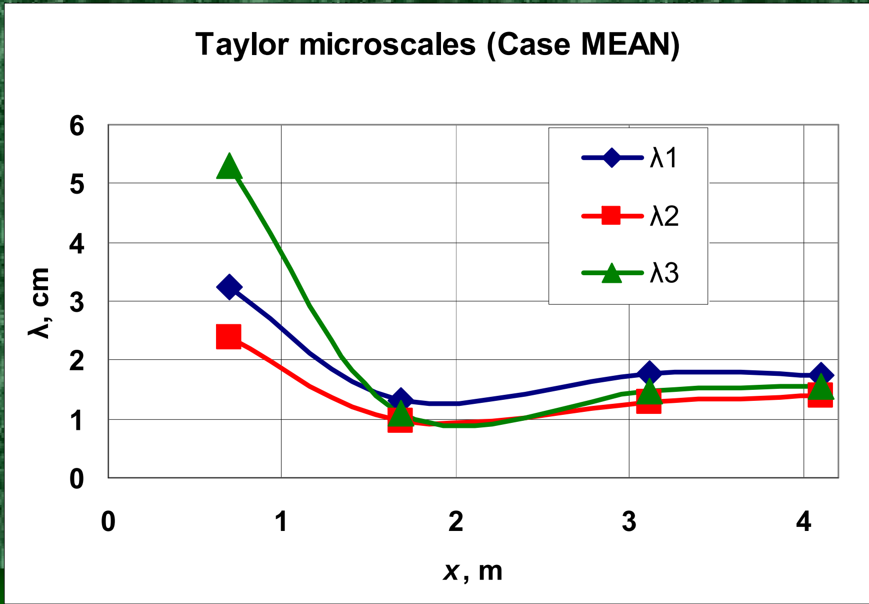

TAYLOR MICRO-SCALE RE

Grid 1- Tr 28

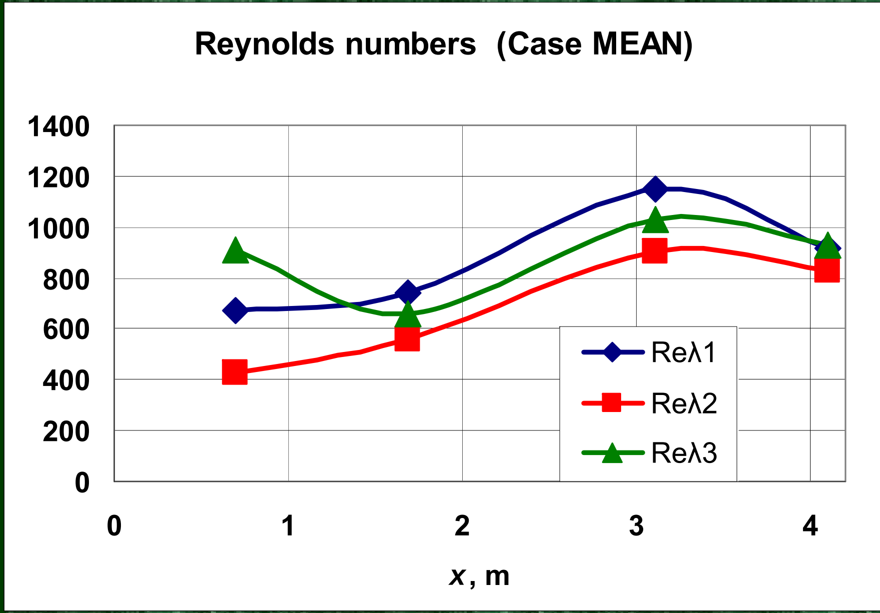

Grid 2- Tr 17

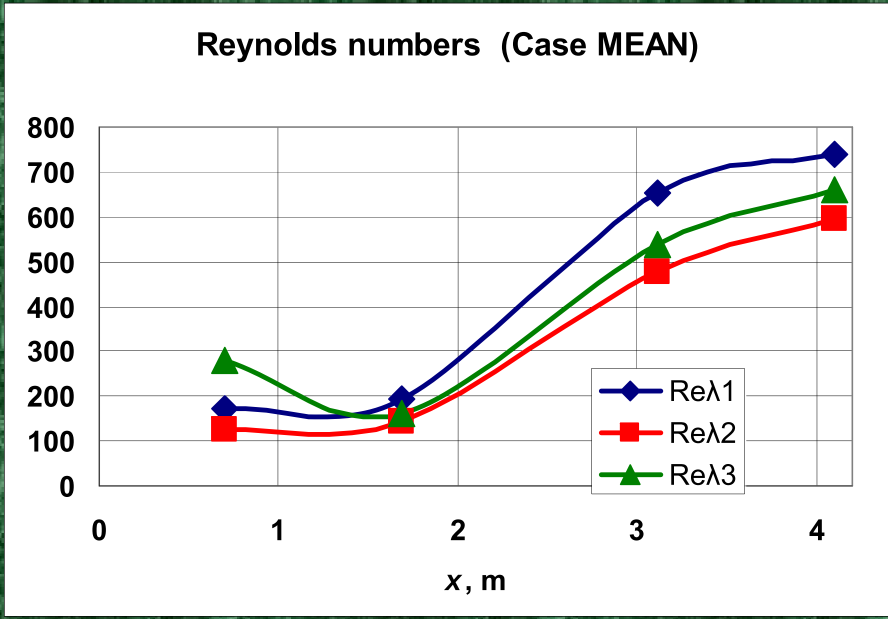

ENERGY DISSIPATION

Grid 1- Tr 28

Grid 2- Tr 17

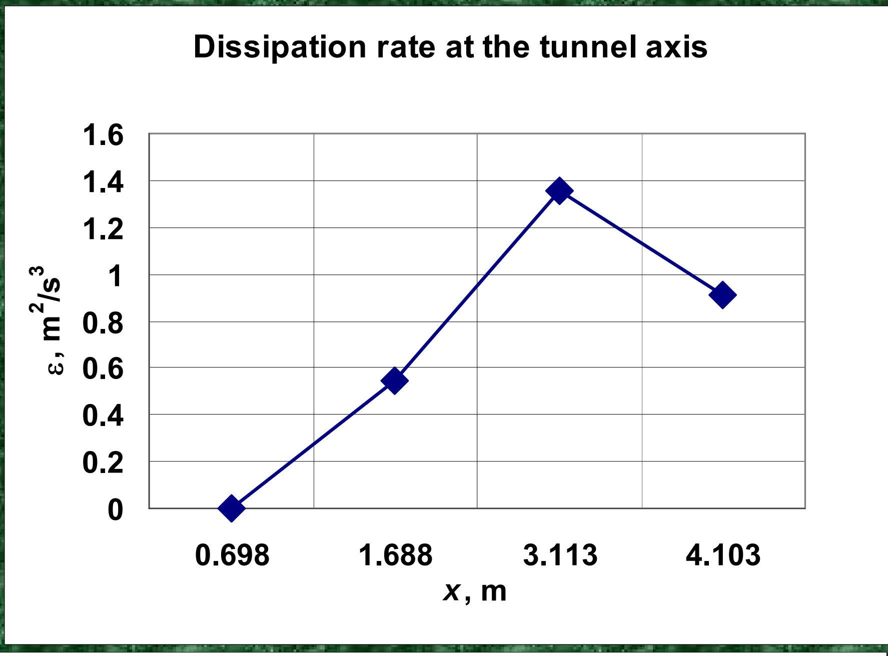

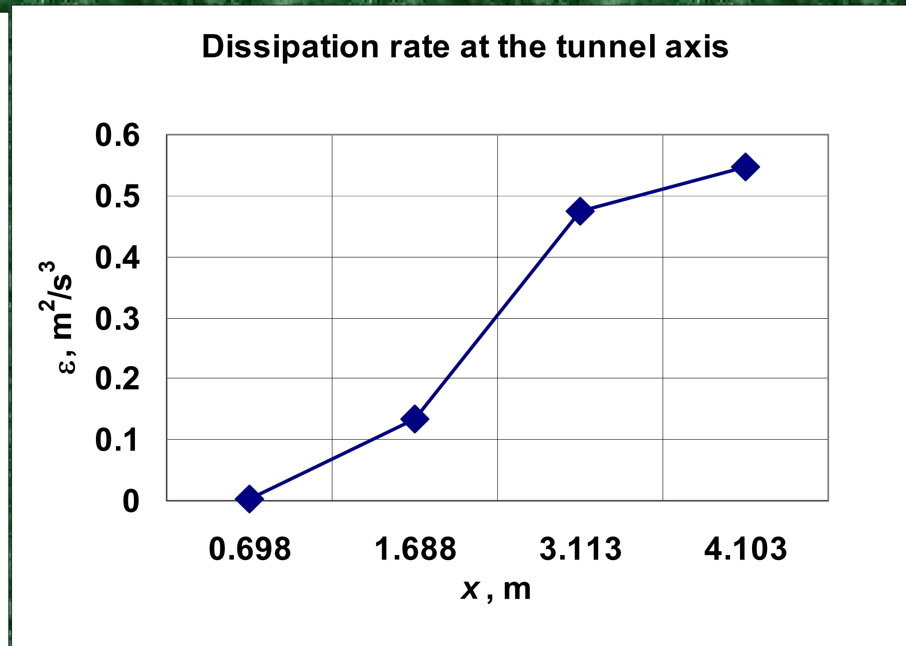

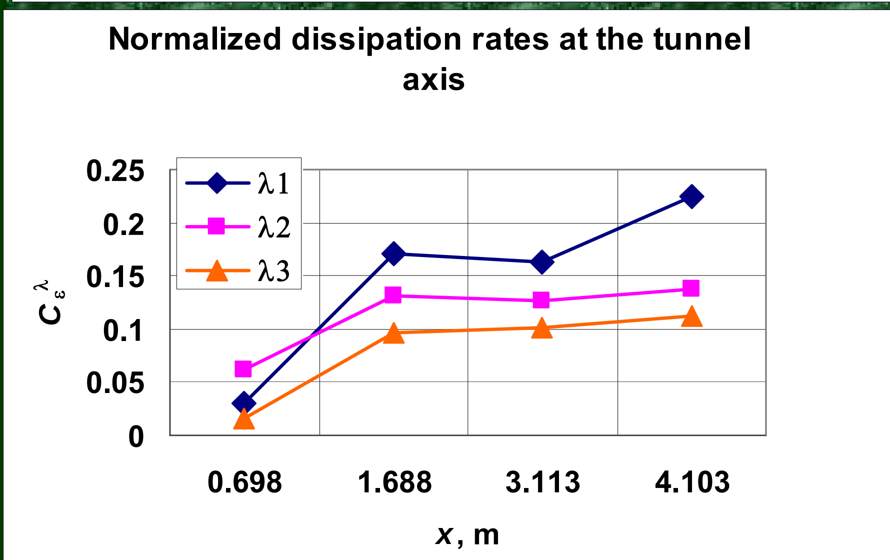

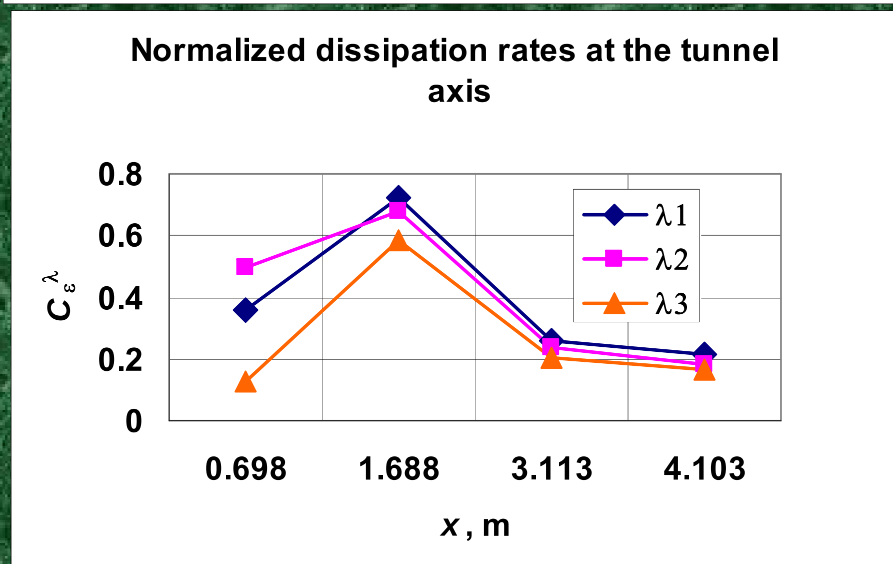

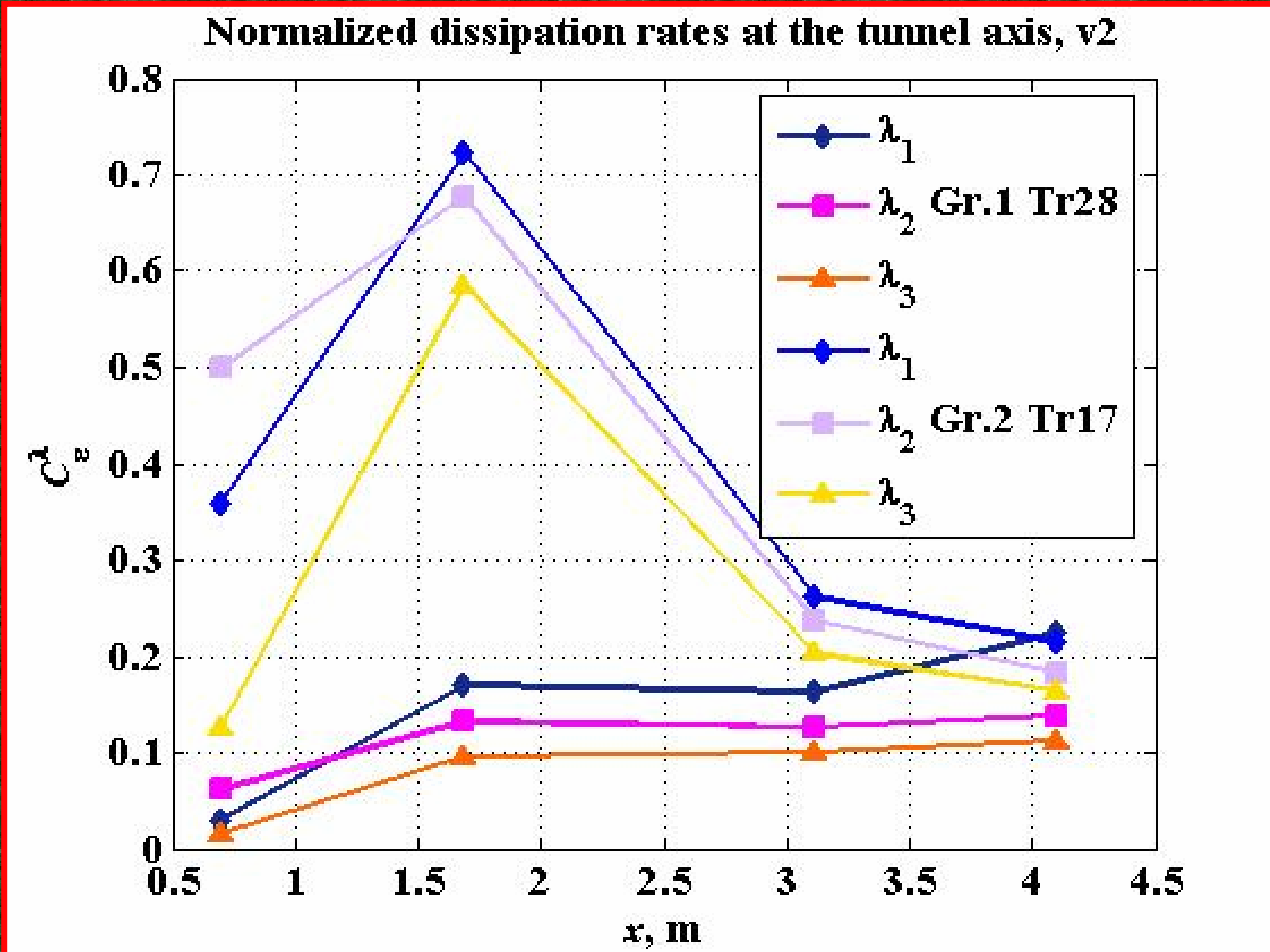
Normalized dissipation rates at the tunnel axis, v2
C_ε^λ
x, m
0
0.1
0.2
0.3
0.4
0.5
0.6
0.7
0.8
0.5
1
1.5
2
2.5
3
3.5
4
4.5
λ_1
λ_2 Gr.1 Tr28
λ_3
λ_1
λ_2 Gr.2 Tr17
λ_3

THIRD ORDER MOMENTS

Grid 1- Tr 28 **Grid 2- Tr 17**

Skewness

$\frac{\partial u_1}{\partial x_1}$	$\frac{\partial u_2}{\partial x_2}$	$\frac{\partial u_3}{\partial x_3}$	$\frac{\partial u_i}{\partial x_k},\ i \neq k$	$\frac{\langle \omega_i \omega_k s_{ik} \rangle}{\langle \omega^2 \rangle^{3/2}}$	$\frac{\langle s_{ij} s_{jk} s_{ki} \rangle}{\langle s^2 \rangle^{3/2}}$
0.73	0.65	0.65	$0.05 \div 0.1$	0.18	0.38
				$(0.21)_{S_{\frac{\partial u_1}{\partial x_1}} = 0.7}$	$(0.42)_{S_{\frac{\partial u_1}{\partial x_1}} = 0.7}$

$Re_\lambda \sim 10^4$ Field experiment

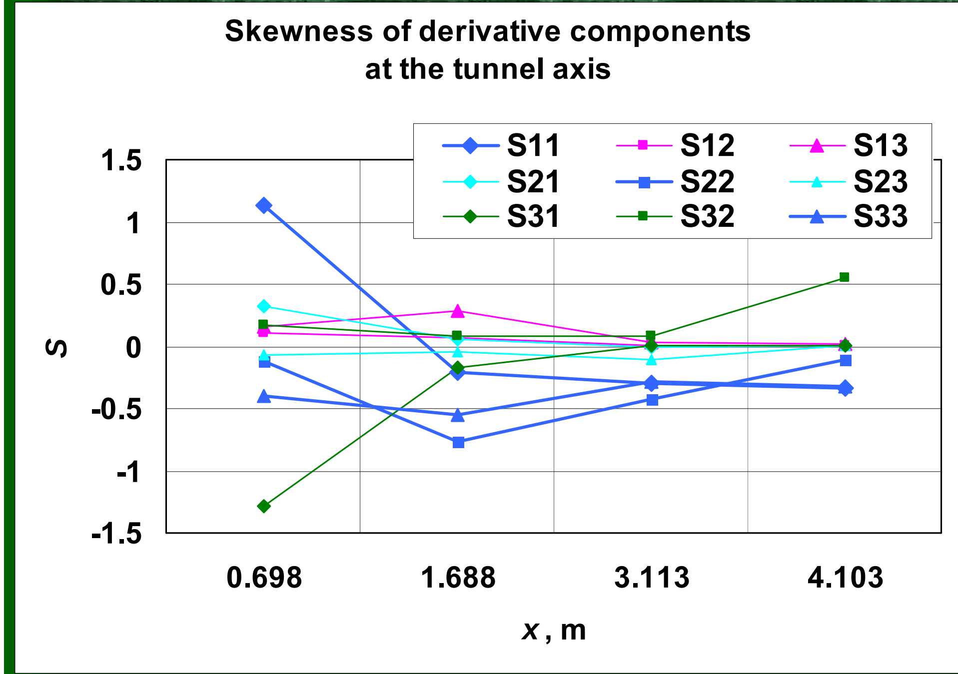

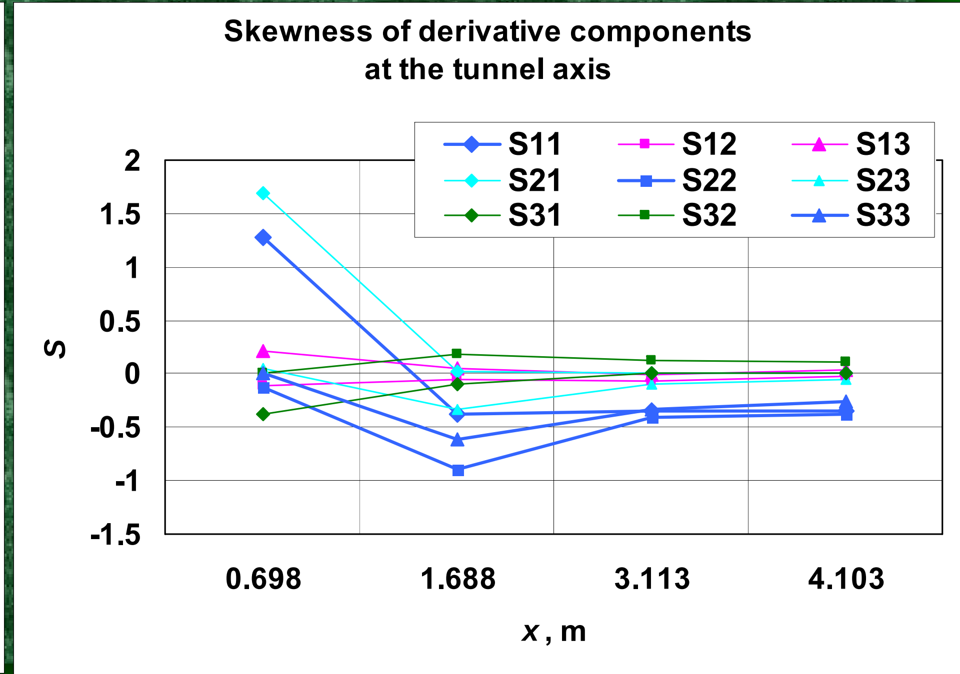

THIRD ORDER MOMENTS

Grid 1- Tr 28

Grid 2- Tr 17

Skewness

$\frac{\partial u_1}{\partial x_1}$	$\frac{\partial u_2}{\partial x_2}$	$\frac{\partial u_3}{\partial x_3}$	$\frac{\partial u_i}{\partial x_k},\ i \neq k$	$\frac{\langle \omega_i \omega_k s_{ik} \rangle}{\langle \omega^2 \rangle^{3/2}}$	
0.73	0.65	0.65	$0.05 \div 0.1$	0.18	**0.1**
				$(0.21)_{S_{\frac{\partial u_1}{\partial x_1}}=0.7}$	

Re$_\lambda$~10^4 Field experiment

Re$_\lambda$~10^2 grid

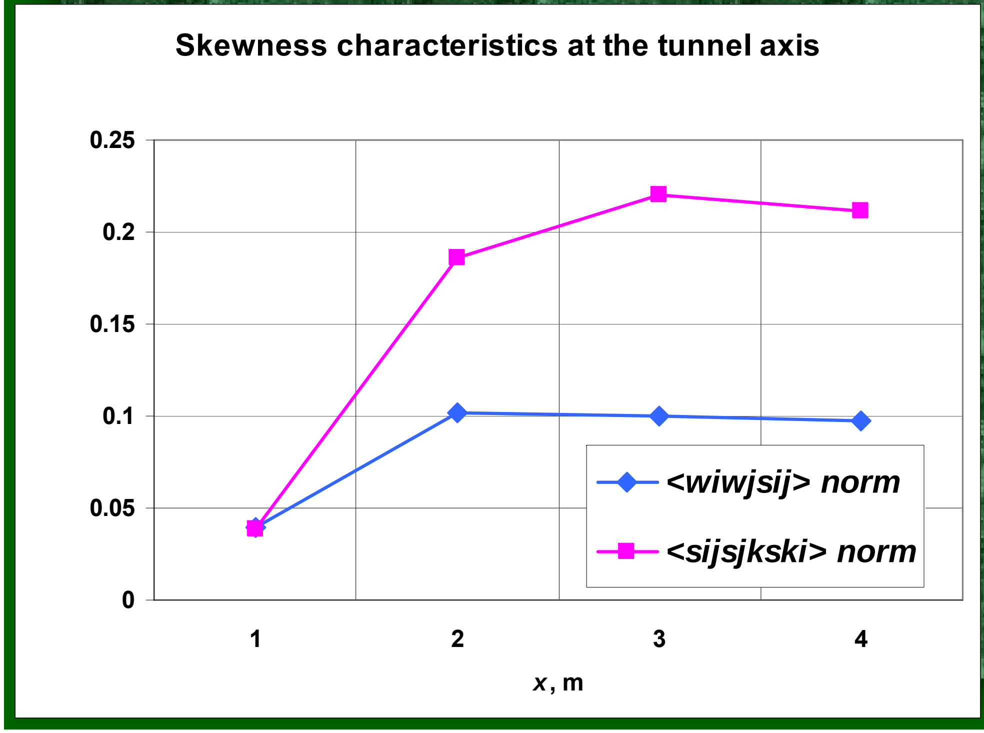

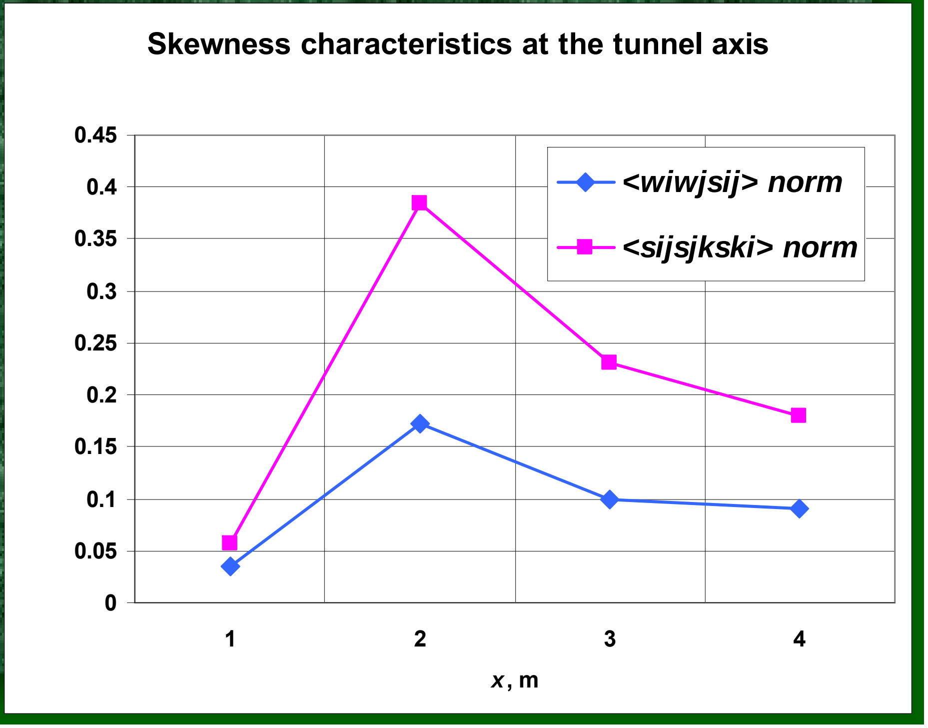

FOURTH ORDER MOMENTS

Grid 1- Tr 28

Grid 2- Tr 17

Flattness

Re_λ~10^4 Field experiment

	$\frac{\partial u_i}{\partial x_k}$	$\frac{15}{7}\frac{\langle s^4\rangle}{\langle s^2\rangle^2}$	$\frac{9}{5}\frac{\langle \omega^4\rangle}{\langle \omega^2\rangle^2}$	$\frac{\langle \omega^2 s^2\rangle}{\langle \omega^2\rangle\langle s^2\rangle}$	$3\frac{\langle(\omega_k s_{ik})^2\rangle}{\langle \omega^2\rangle\langle s^2\rangle}$
Real	$20 \div 25$	17.5	27.6	6.7	3.6
Gaussian	3	3	3	1	1

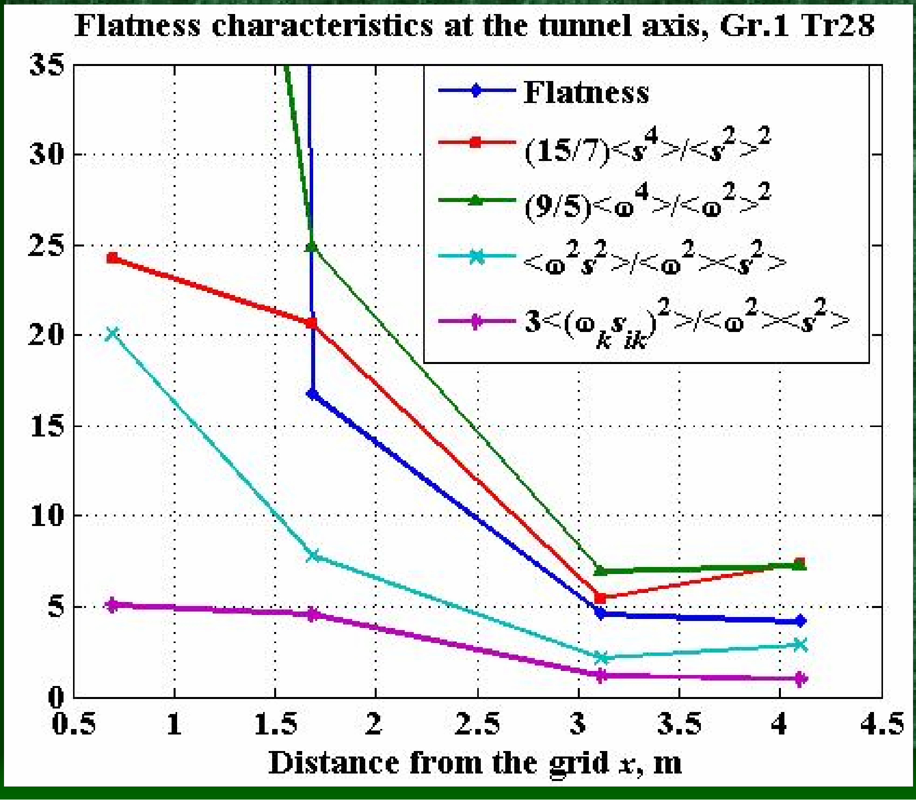

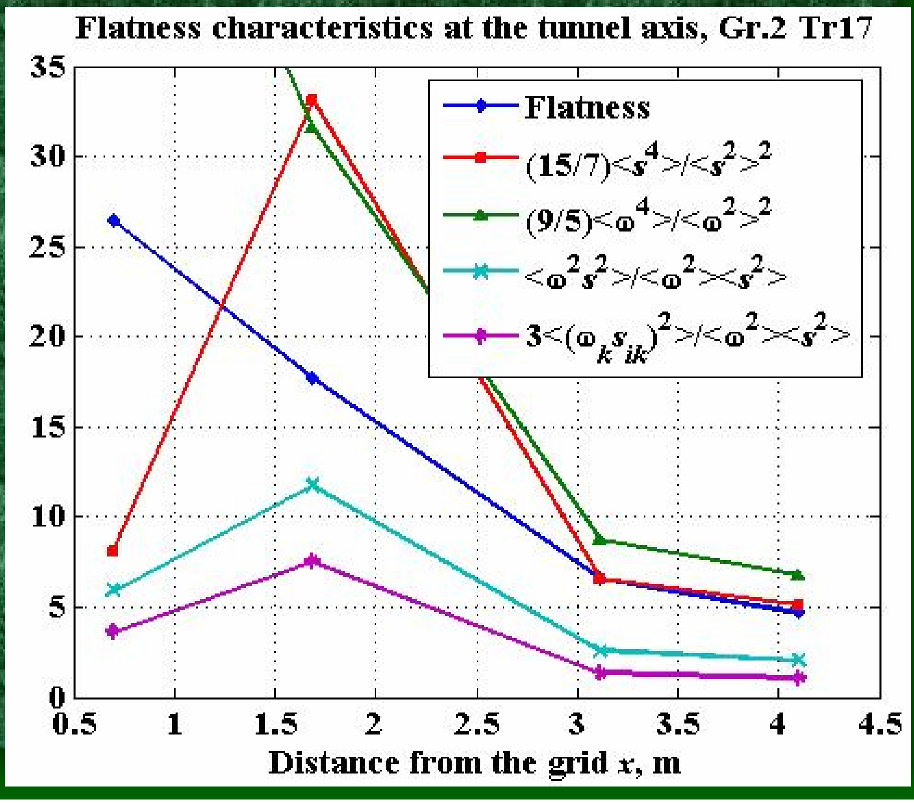

$Re_\lambda \sim 10^2$ Grid experiment 1992

x/M	8	17	30	38	64	90	B. layer y/δ	
							0.7	0.2
S_1	0.41	0.46	0.50	0.50	0.50	0.50	0.56	0.35
S_2	0.32	0.41	0.44	0.55	0.40	0.37	0.32	0.045
S_3	0.31	0.34	0.38	0.33	0.20	0.14	0.68	-1.61
S	0.12	0.13	0.16	0.16	0.14	0.15	0.16	0.06

TABLE 7. Values of $S_\alpha = -\langle(\partial u_\alpha/\partial x_\alpha)^3\rangle/\langle(\partial u_\alpha/\partial x_\alpha)^2\rangle^{\frac{3}{2}}$ and $S = \langle\omega_i\omega_j s_{ij}\rangle/\langle\omega^2\rangle/\langle(s_{ij}s_{ij})\rangle^{\frac{1}{2}}$

x/M	8	17	30	38	64	90	B. layer y/δ		
							0.7	0.2	Gaussian
F_1	3.97	3.99	4.07	4.27	3.95	3.97	9.09	33.8	3
F_2	4.29	4.42	4.48	4.72	4.62	4.46	11.5	46.4	3
F_3	1.04	0.93	0.88	0.88	0.76	0.82	2.09	3.77	1
F_4	4.77	4.90	5.10	5.30	5.21	4.95	12.3	34.9	3

TABLE 8. Fourth-order moments of velocity derivatives

Fourth moments of velocity derivatives defined as

$$F_1 = \frac{15}{7}\frac{\langle s^4\rangle}{\langle s^2\rangle^2}, \quad F_2 = 3\frac{\langle\omega^2 s^2\rangle}{\langle\omega^2\rangle\langle s^2\rangle}, \quad F_3 = 3\frac{\langle\omega_i s_{ij} s_{jk}\omega_k\rangle}{\langle\omega^2\rangle\langle s^2\rangle}, \quad F_4 = \frac{9}{5}\frac{\langle\omega^4\rangle}{\langle\omega^2\rangle^2},$$

Grid 1- Tr 28

Grid 2- Tr 17

PDFs of Eigenvalues of the Rate of Strain Tensor

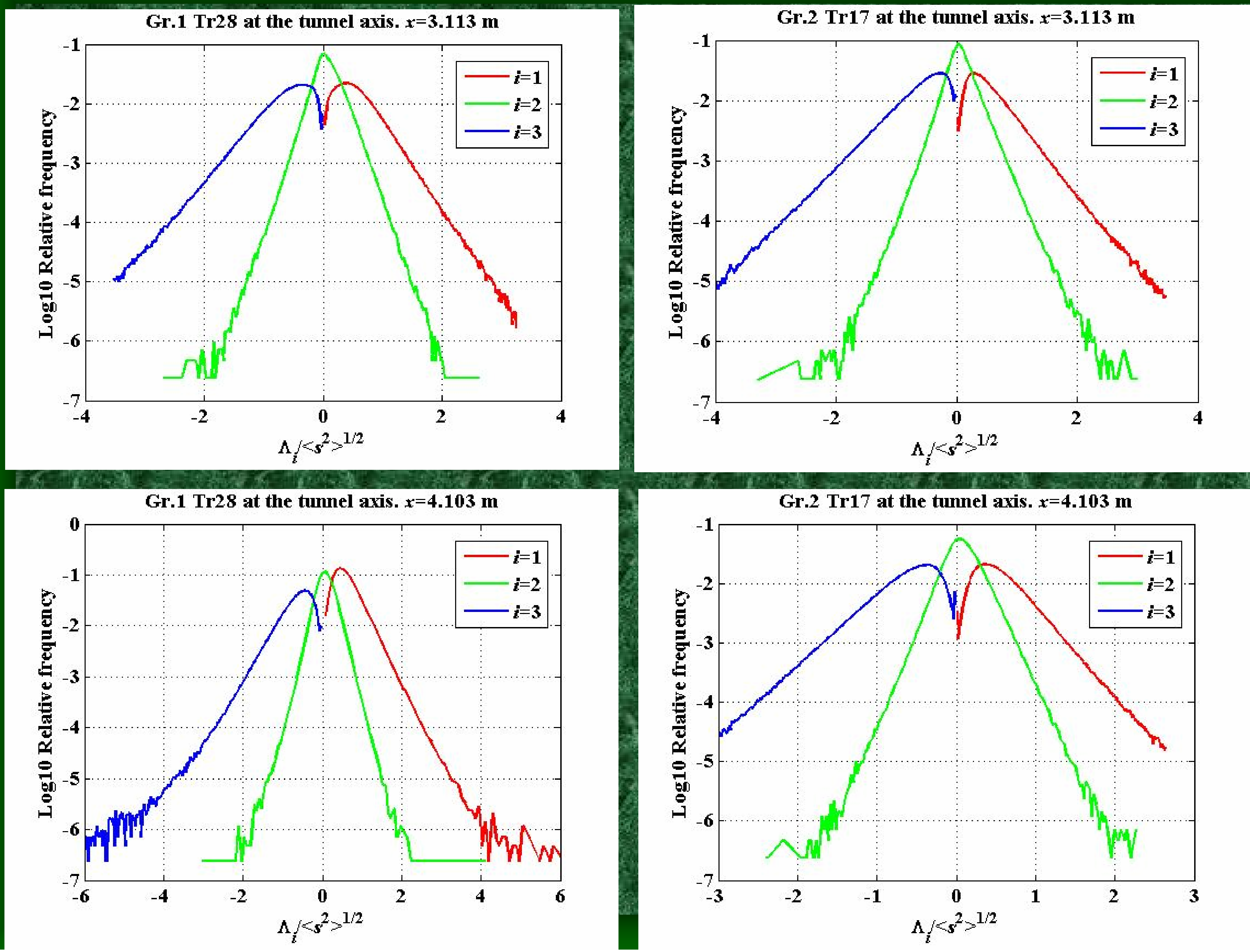
Gr.1 Tr28 at the tunnel axis. x=3.113 m
Gr.2 Tr17 at the tunnel axis. x=3.113 m
Gr.1 Tr28 at the tunnel axis. x=4.103 m
Gr.2 Tr17 at the tunnel axis. x=4.103 m
Log10 Relative frequency
$\Lambda_i/\langle s^2\rangle^{1/2}$
i=1
i=2
i=3

Alignments of Vorticity and the Vortex Stretching Vector, $W_i = \omega_k s_{ik}$

Grid 1- Tr 28

Grid 2- Tr 17

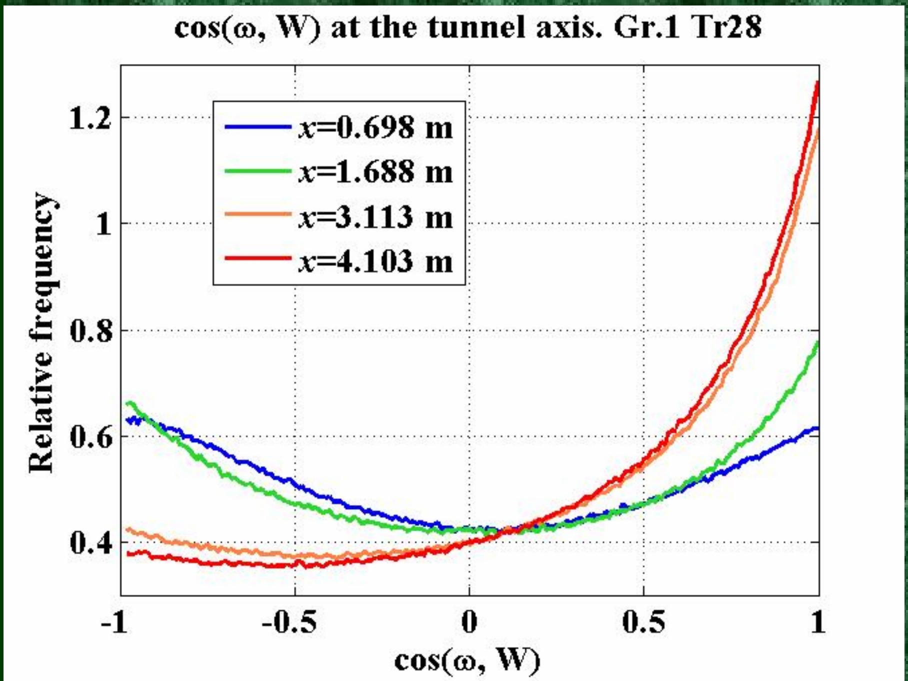

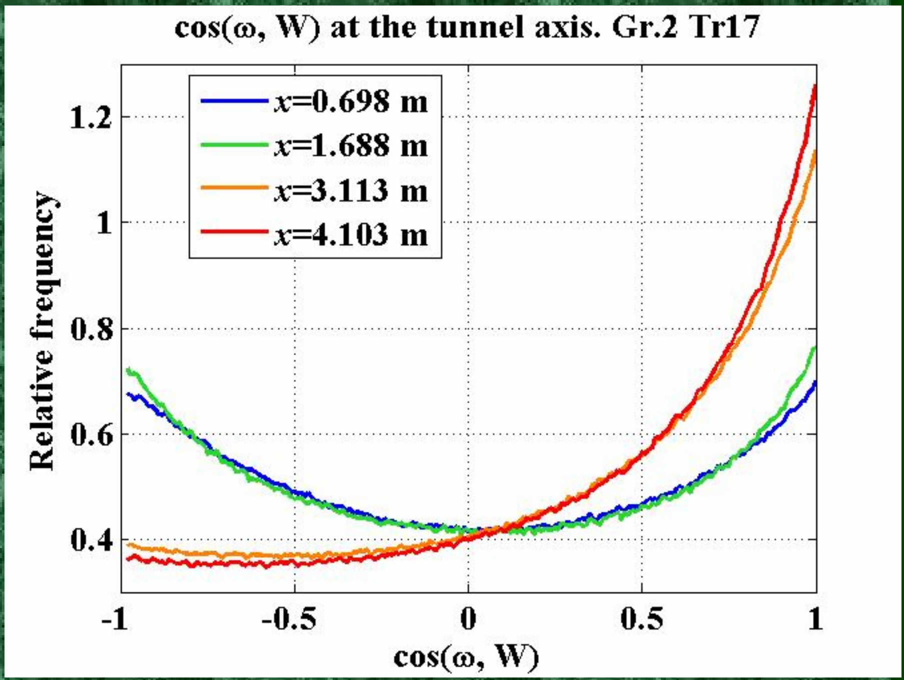

Grid 1- Tr 28

Grid 2- Tr 17

Alignments of Vorticity and Eigen-Frame of the Rate of Strain Tensor

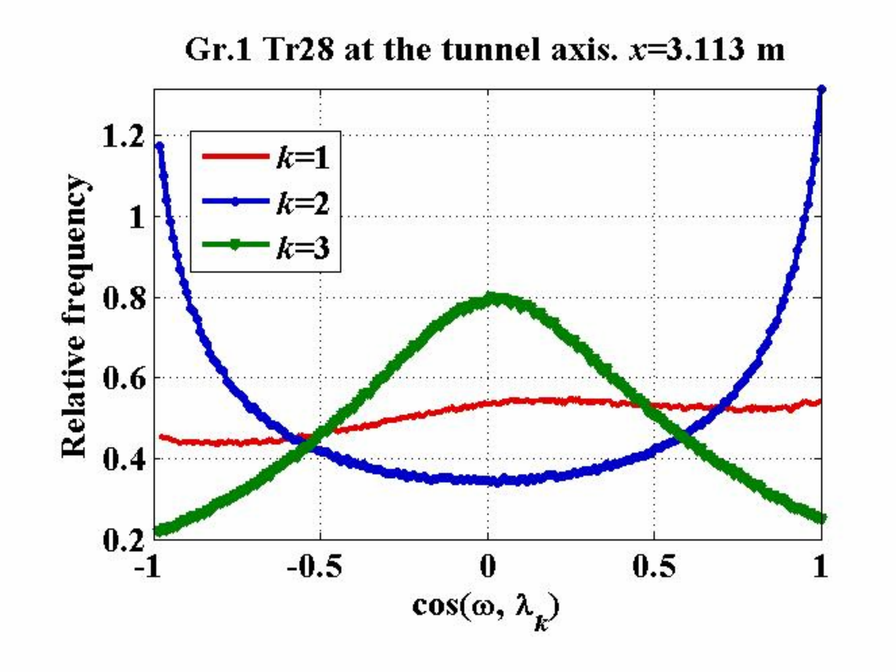
Gr.1 Tr28 at the tunnel axis. x=3.113 m
Relative frequency
$\cos(\omega, \lambda_k)$
k=1
k=2
k=3

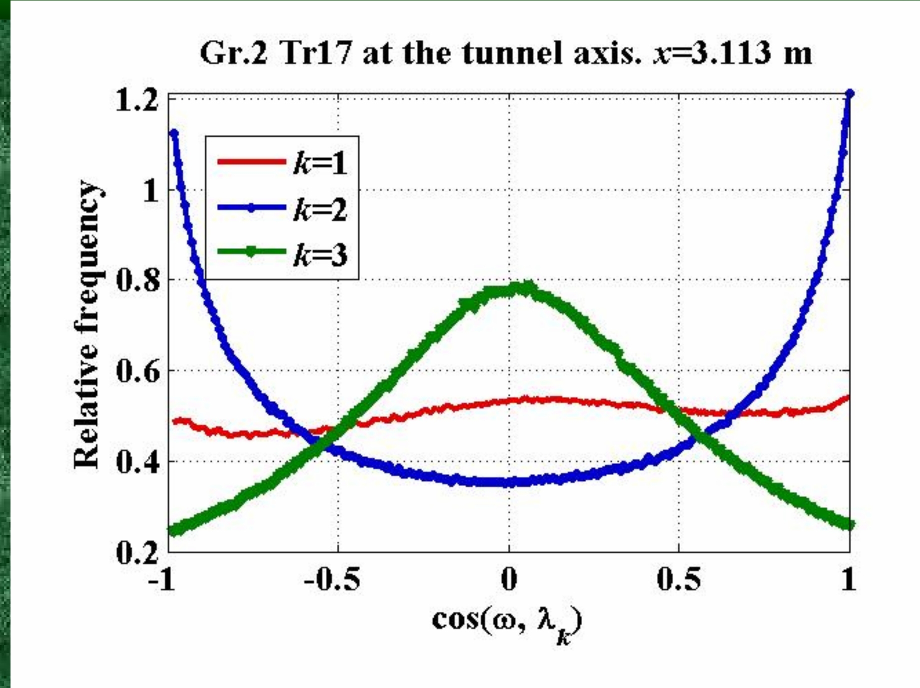
Gr.2 Tr17 at the tunnel axis. x=3.113 m
Relative frequency
$\cos(\omega, \lambda_k)$
k=1
k=2
k=3

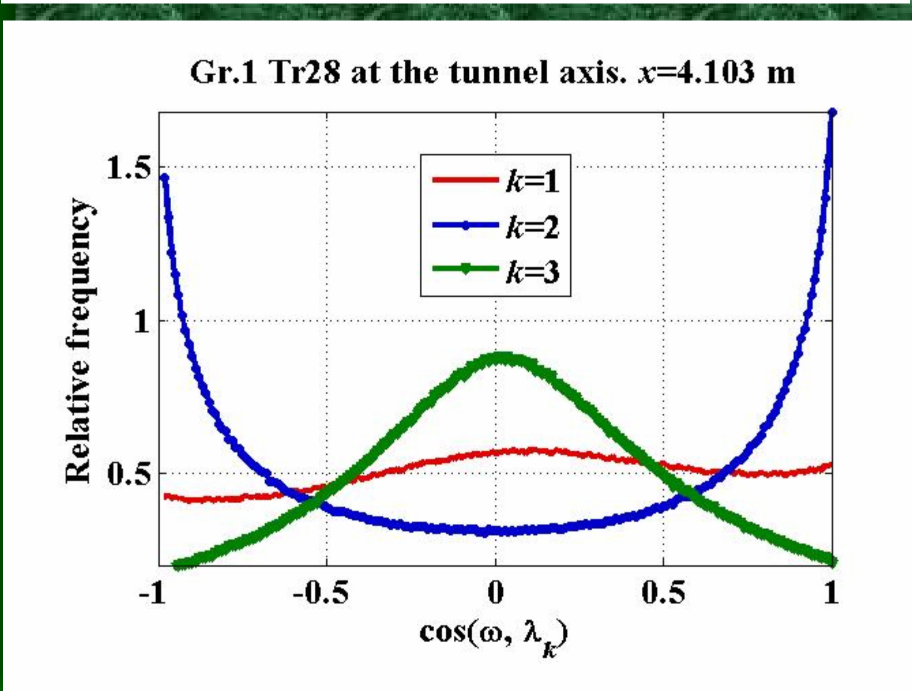
Gr.1 Tr28 at the tunnel axis. x=4.103 m
Relative frequency
$\cos(\omega, \lambda_k)$
k=1
k=2
k=3

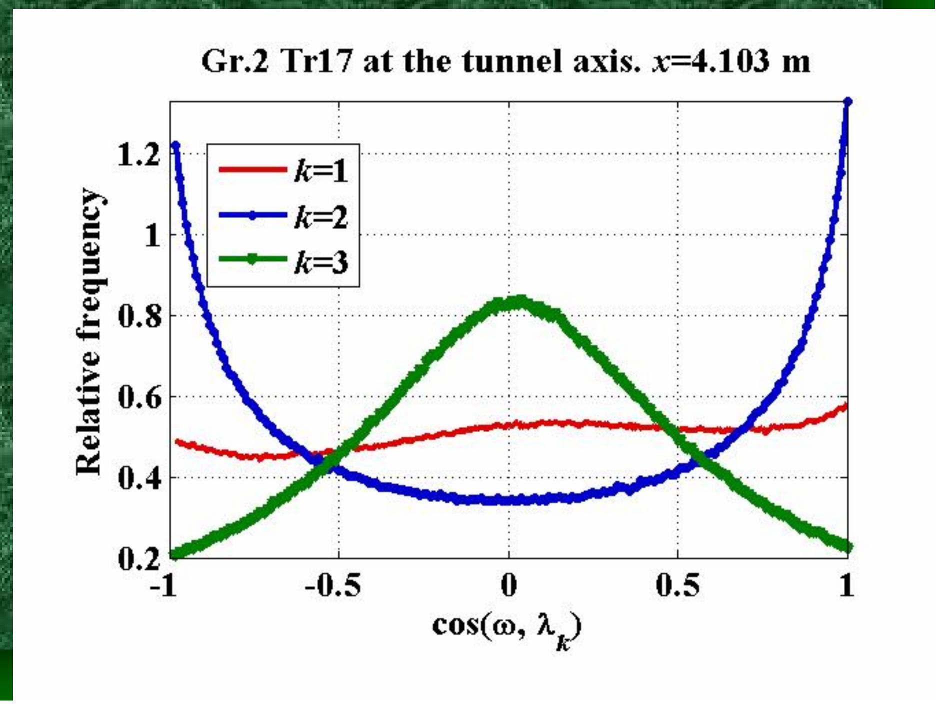
Gr.2 Tr17 at the tunnel axis. x=4.103 m
Relative frequency
$\cos(\omega, \lambda_k)$
k=1
k=2
k=3

Grid 1- Tr 28 Grid 2- Tr 17

PDFs of Enstrophy and Strain Production

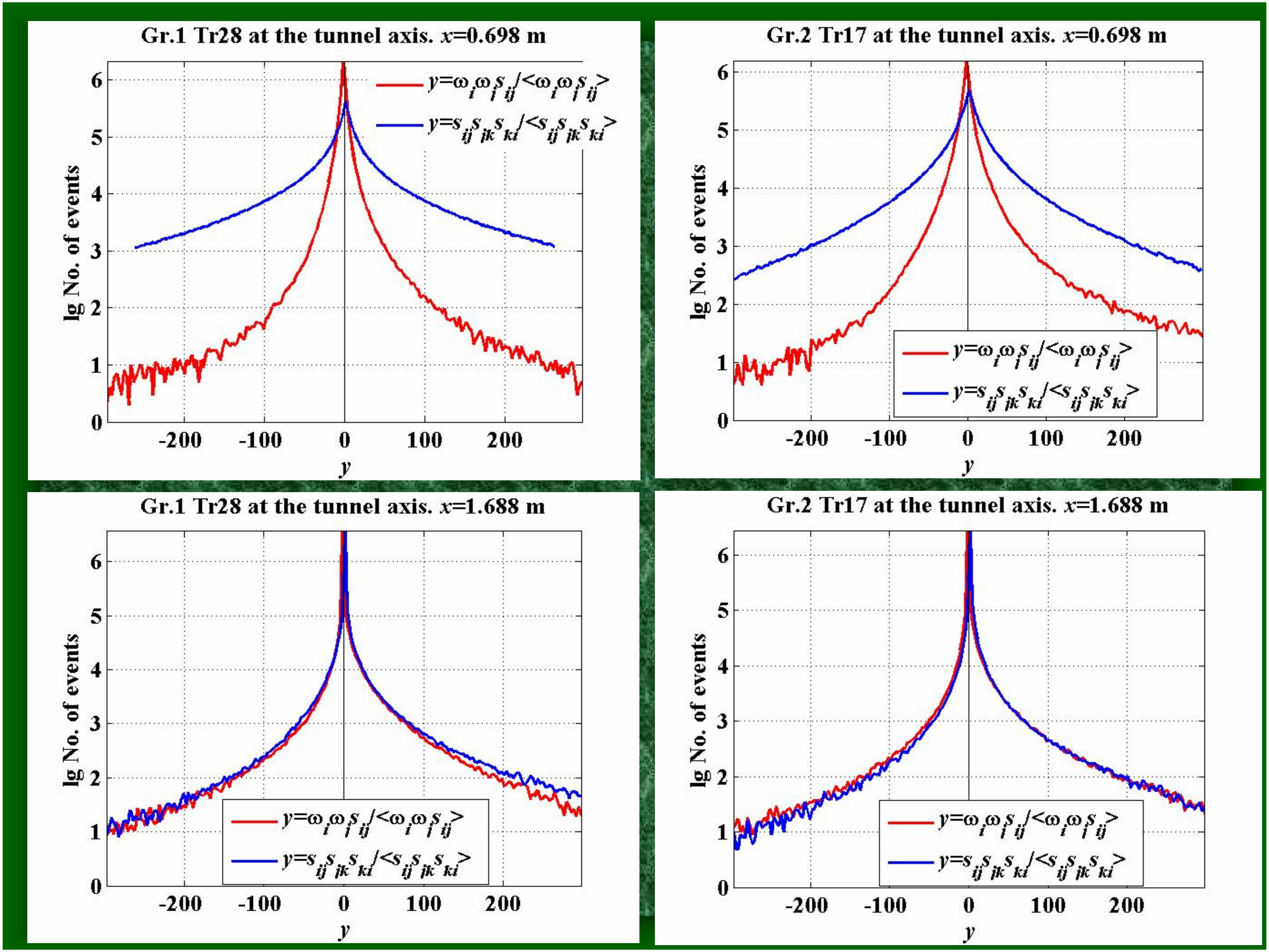

Gr.1 Tr28 at the tunnel axis. x=0.698 m
Gr.2 Tr17 at the tunnel axis. x=0.698 m
Gr.1 Tr28 at the tunnel axis. x=1.688 m
Gr.2 Tr17 at the tunnel axis. x=1.688 m
$y=\omega_i\omega_j s_{ij}/<\omega_i\omega_j s_{ij}>$
$y=s_{ij}s_{jk}s_{ki}/<s_{ij}s_{jk}s_{ki}>$
lg No. of events
y

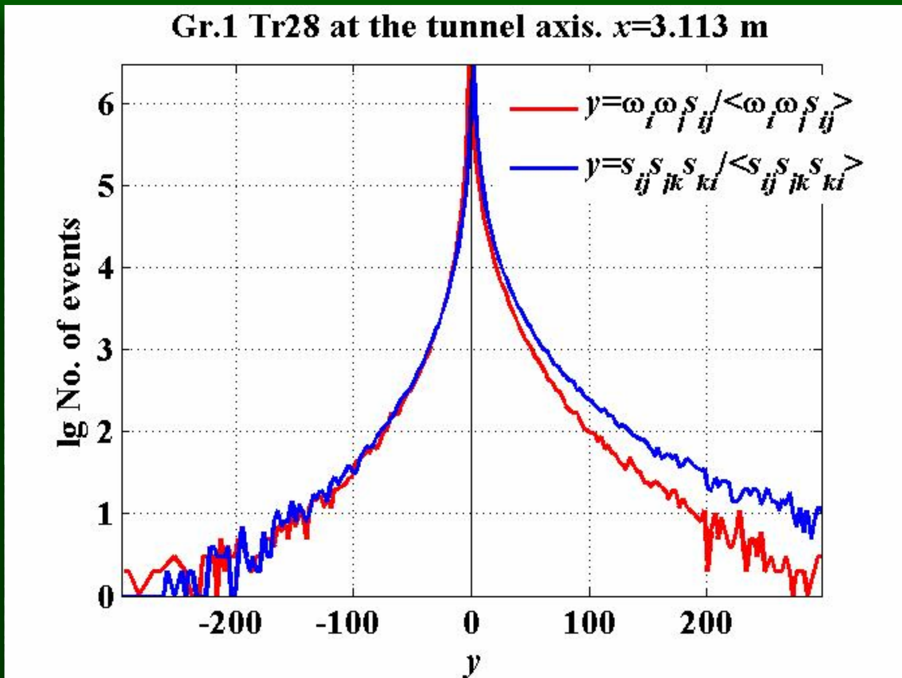
Gr.1 Tr28 at the tunnel axis. x=3.113 m
$y=\omega_i\omega_j s_{ij}/\langle\omega_i\omega_j s_{ij}\rangle$
$y=s_{ij}s_{jk}s_{ki}/\langle s_{ij}s_{jk}s_{ki}\rangle$
lg No. of events
y

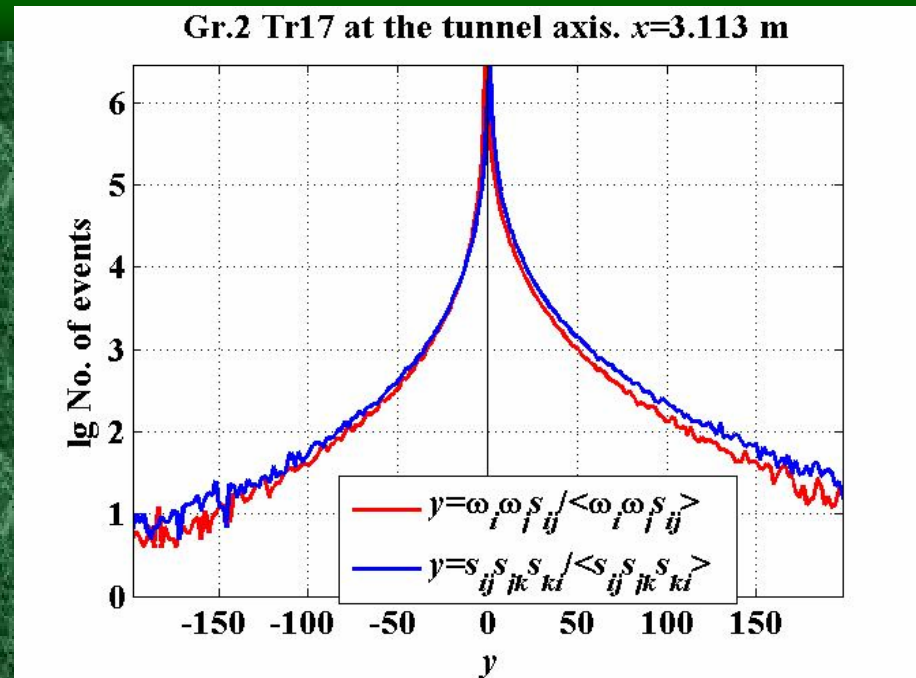
Gr.2 Tr17 at the tunnel axis. x=3.113 m
$y=\omega_i\omega_j s_{ij}/\langle\omega_i\omega_j s_{ij}\rangle$
$y=s_{ij}s_{jk}s_{ki}/\langle s_{ij}s_{jk}s_{ki}\rangle$
lg No. of events
y

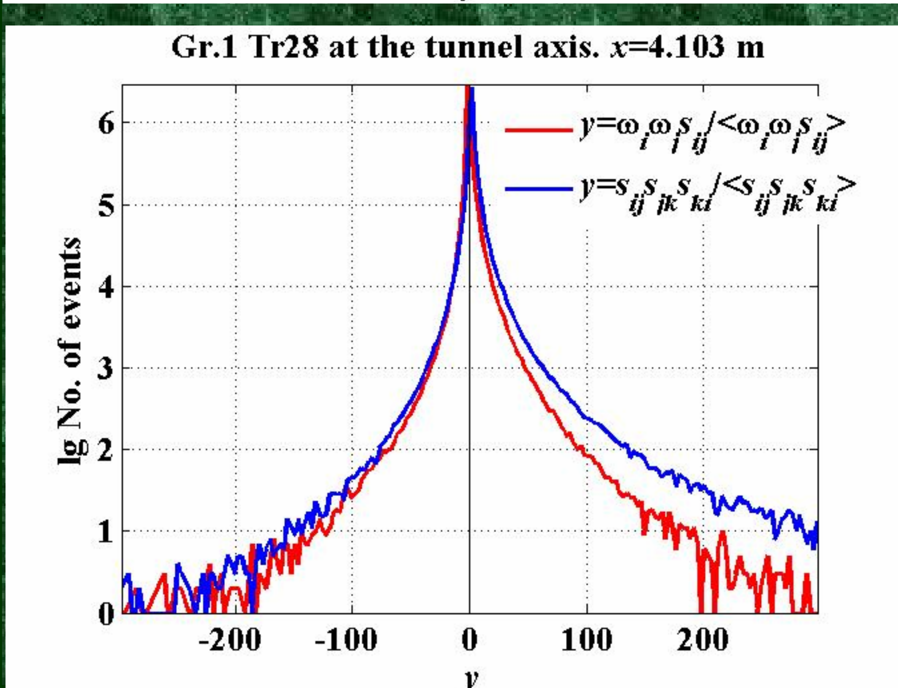
Gr.1 Tr28 at the tunnel axis. x=4.103 m
$y=\omega_i\omega_j s_{ij}/\langle\omega_i\omega_j s_{ij}\rangle$
$y=s_{ij}s_{jk}s_{ki}/\langle s_{ij}s_{jk}s_{ki}\rangle$
lg No. of events
y

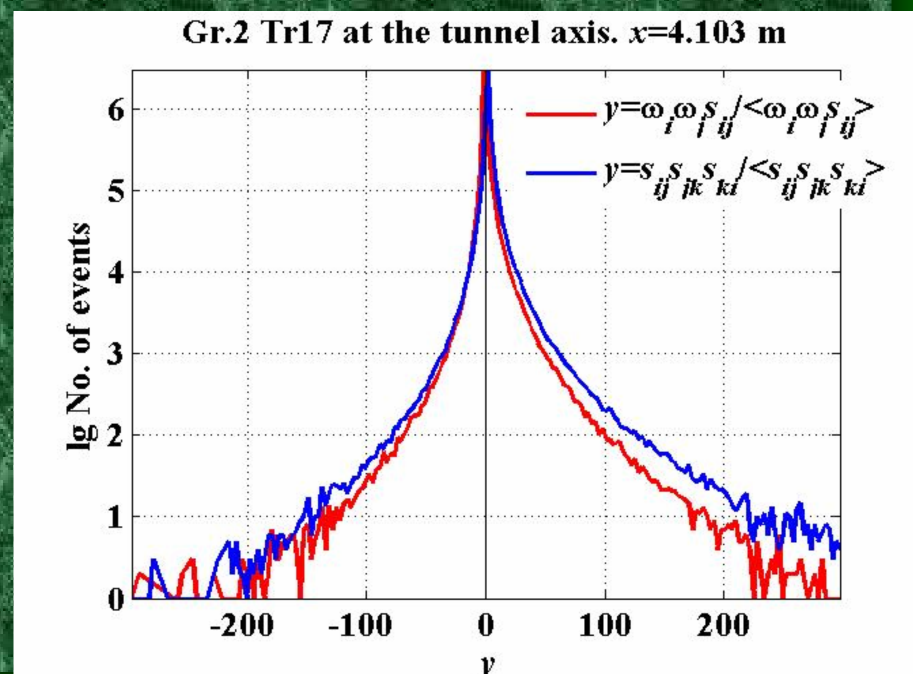
Gr.2 Tr17 at the tunnel axis. x=4.103 m
$y=\omega_i\omega_j s_{ij}/\langle\omega_i\omega_j s_{ij}\rangle$
$y=s_{ij}s_{jk}s_{ki}/\langle s_{ij}s_{jk}s_{ki}\rangle$
lg No. of events
y

Grid 1- Tr 28

Grid 2- Tr 17

PDFs OF VELOCITY DERIVATIVES

$\partial u_i / \partial x_k$

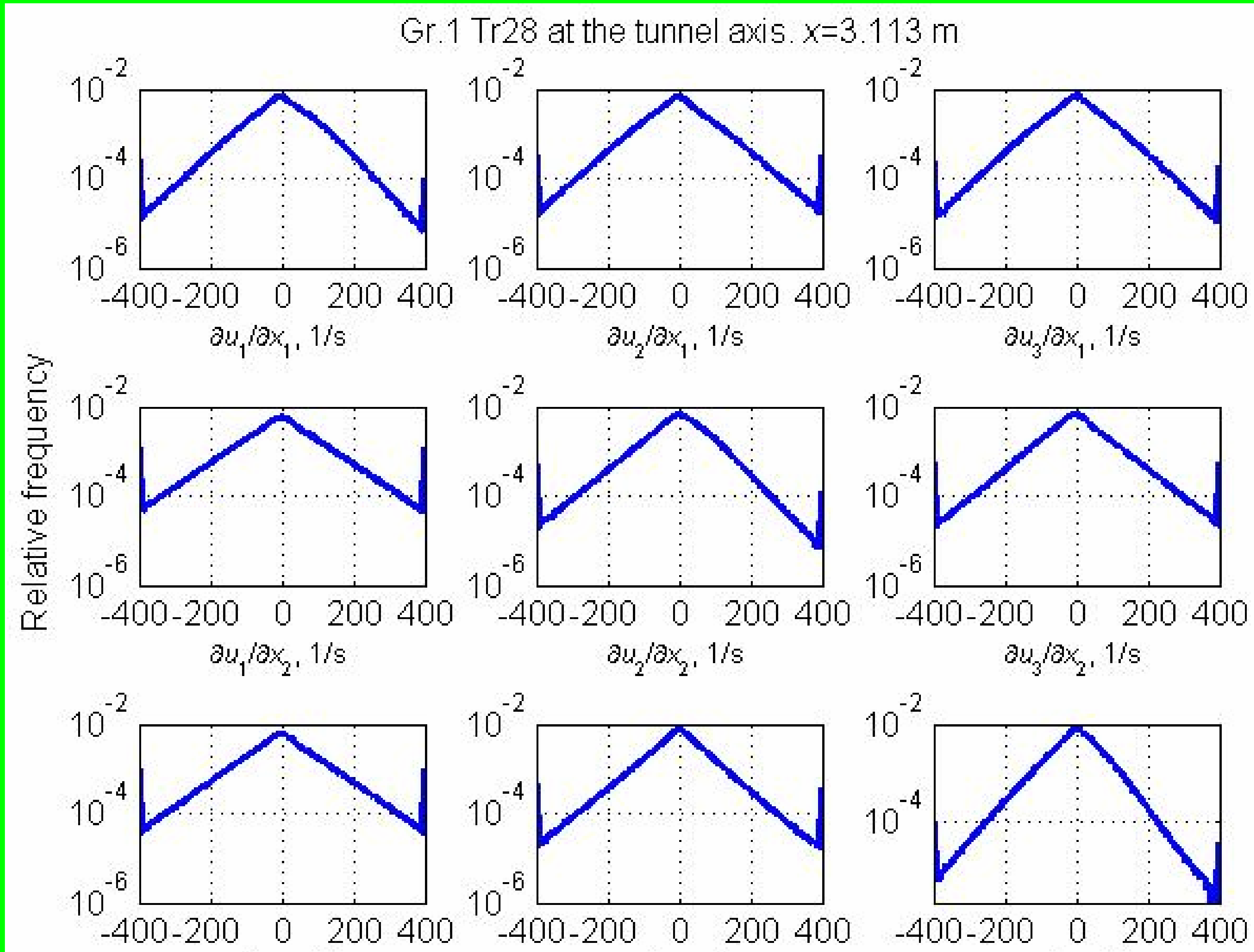

Gr.1 Tr28 at the tunnel axis. x=3.113 m
Relative frequency
10^{-2}
10^{-4}
10^{-6}
-400 -200 0 200 400
$\partial u_1/\partial x_1$, 1/s
$\partial u_2/\partial x_1$, 1/s
$\partial u_3/\partial x_1$, 1/s
$\partial u_1/\partial x_2$, 1/s
$\partial u_2/\partial x_2$, 1/s
$\partial u_3/\partial x_2$, 1/s

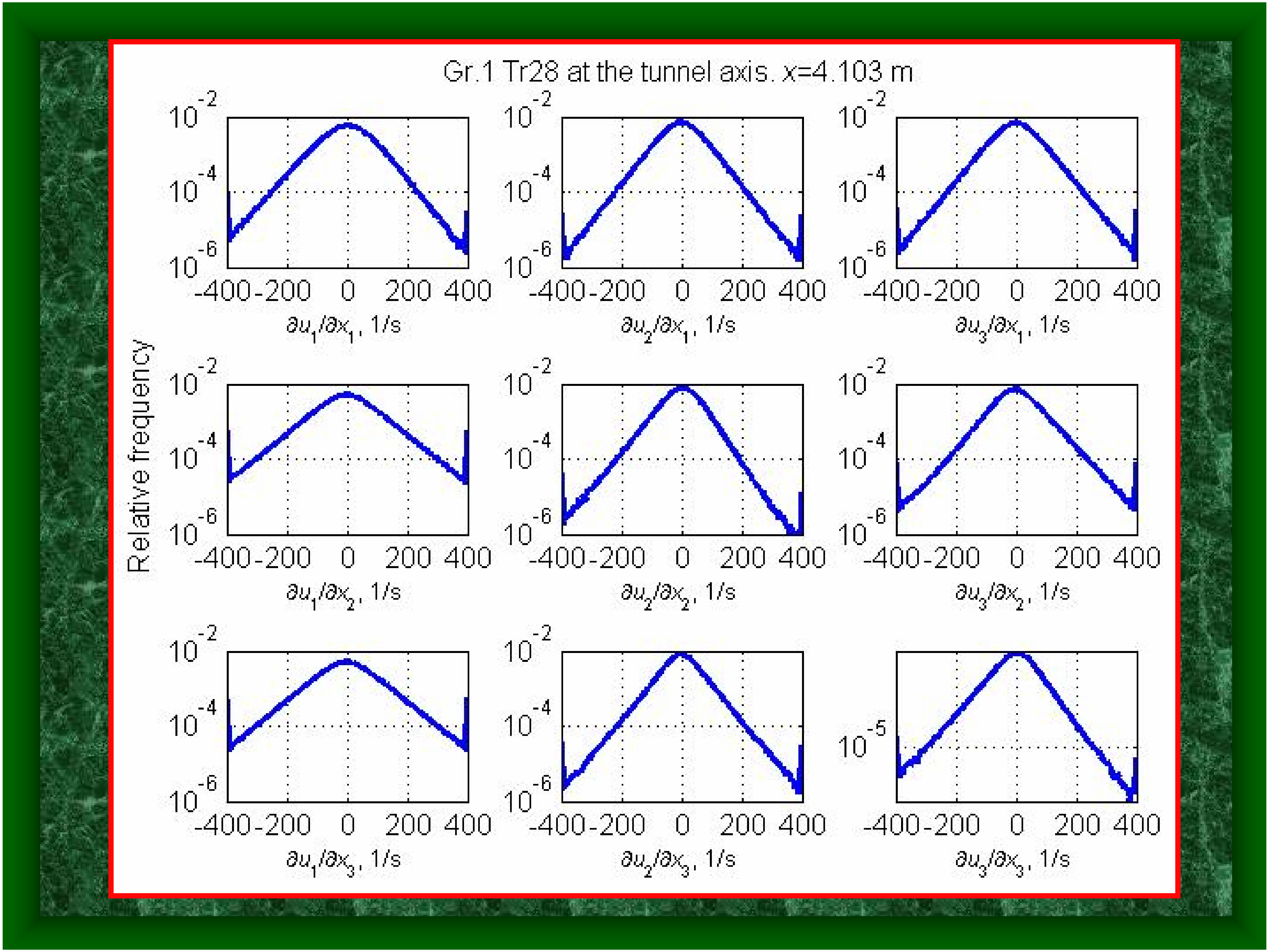

Gr.1 Tr28 at the tunnel axis. x=4.103 m
Relative frequency
∂u1/∂x1, 1/s
∂u2/∂x1, 1/s
∂u3/∂x1, 1/s
∂u1/∂x2, 1/s
∂u2/∂x2, 1/s
∂u3/∂x2, 1/s
∂u1/∂x3, 1/s
∂u2/∂x3, 1/s
∂u3/∂x3, 1/s

Grid 1- Tr 28

Grid 2- Tr 17

JOINT PDFS OF ENSTROPHY AND RATE OF STRAIN PRODUCTION

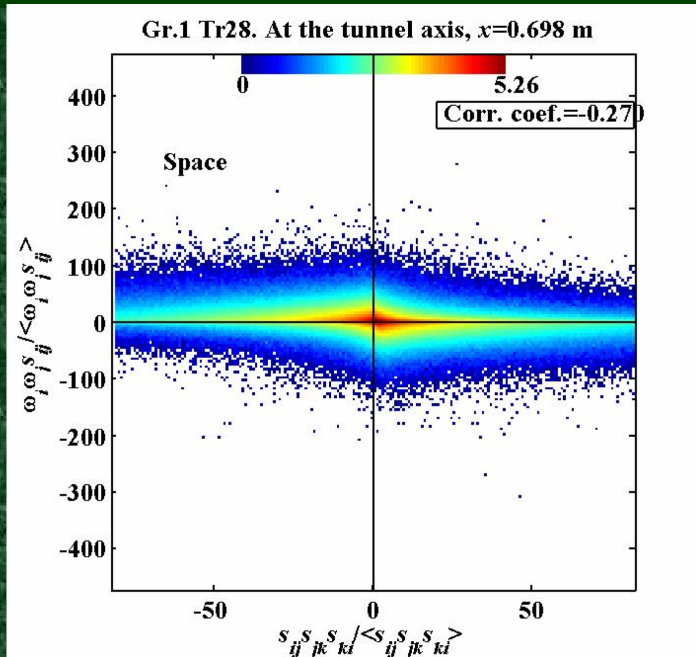
Gr.1 Tr28. At the tunnel axis, x=0.698 m
0
5.26
Corr. coef.=-0.270
Space

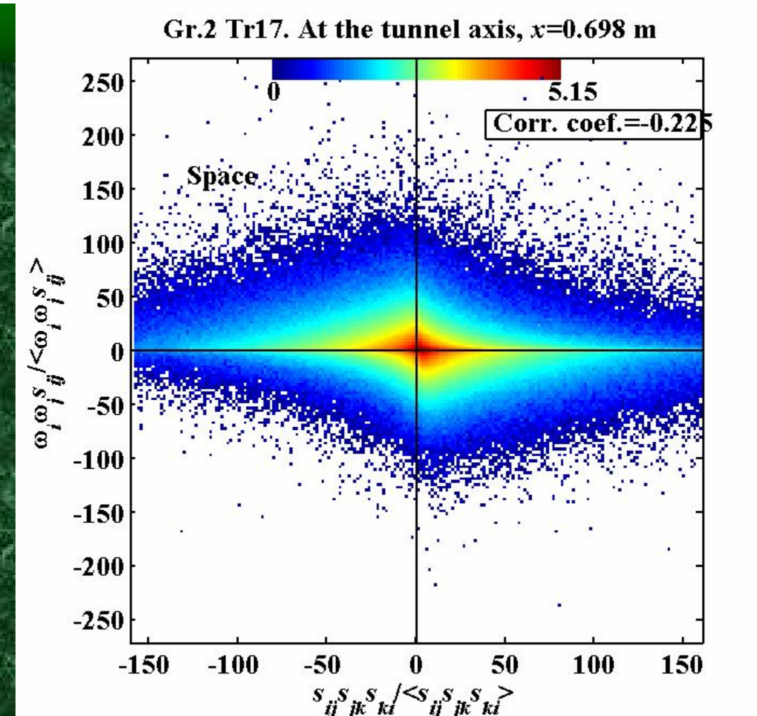
Gr.2 Tr17. At the tunnel axis, x=0.698 m
0
5.15
Corr. coef.=-0.225
Space

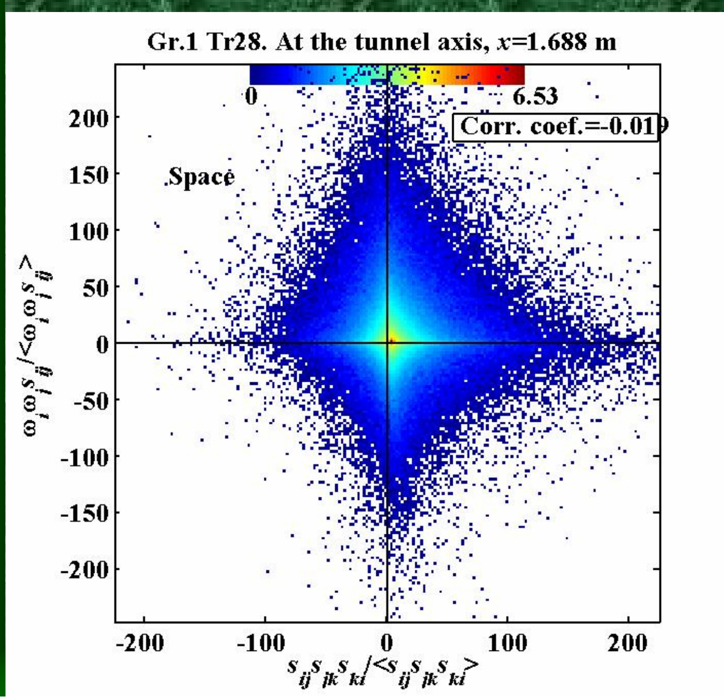
Gr.1 Tr28. At the tunnel axis, x=1.688 m
0
6.53
Corr. coef.=-0.019
Space

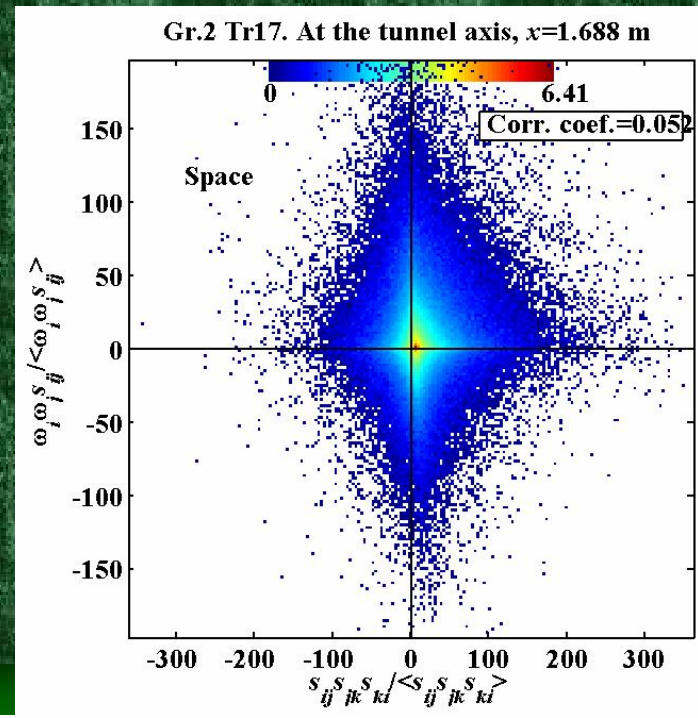
Gr.2 Tr17. At the tunnel axis, x=1.688 m
0
6.41
Corr. coef.=0.052
Space

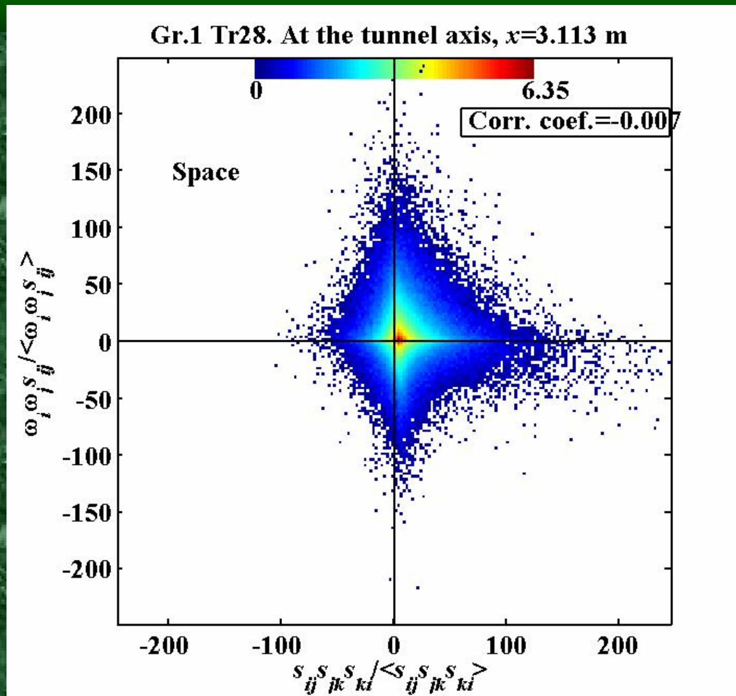
Gr.1 Tr28. At the tunnel axis, x=3.113 m
0
6.35
Corr. coef.=-0.007
Space
$\omega_i\omega_j s_{ij}/\langle\omega_i\omega_j s_{ij}\rangle$
$s_{ij}s_{jk}s_{ki}/\langle s_{ij}s_{jk}s_{ki}\rangle$

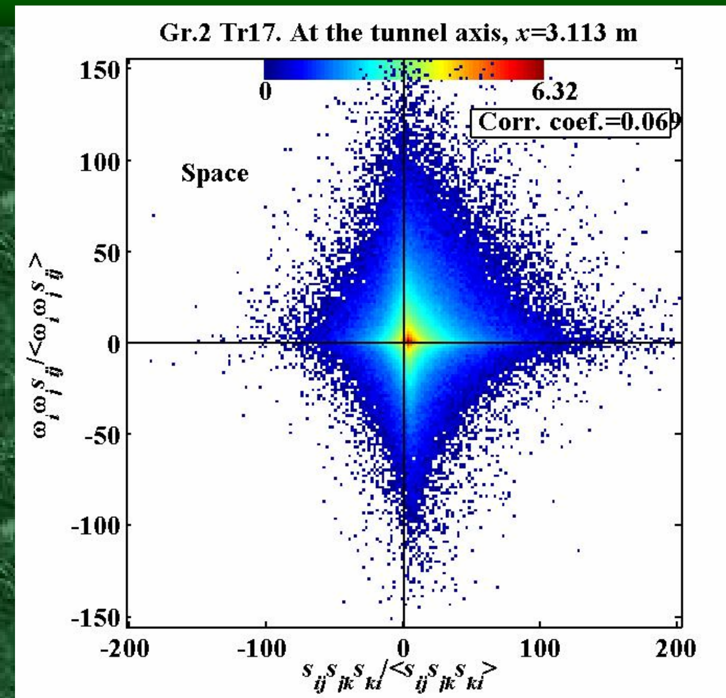
Gr.2 Tr17. At the tunnel axis, x=3.113 m
0
6.32
Corr. coef.=0.069
Space
$\omega_i\omega_j s_{ij}/\langle\omega_i\omega_j s_{ij}\rangle$
$s_{ij}s_{jk}s_{ki}/\langle s_{ij}s_{jk}s_{ki}\rangle$

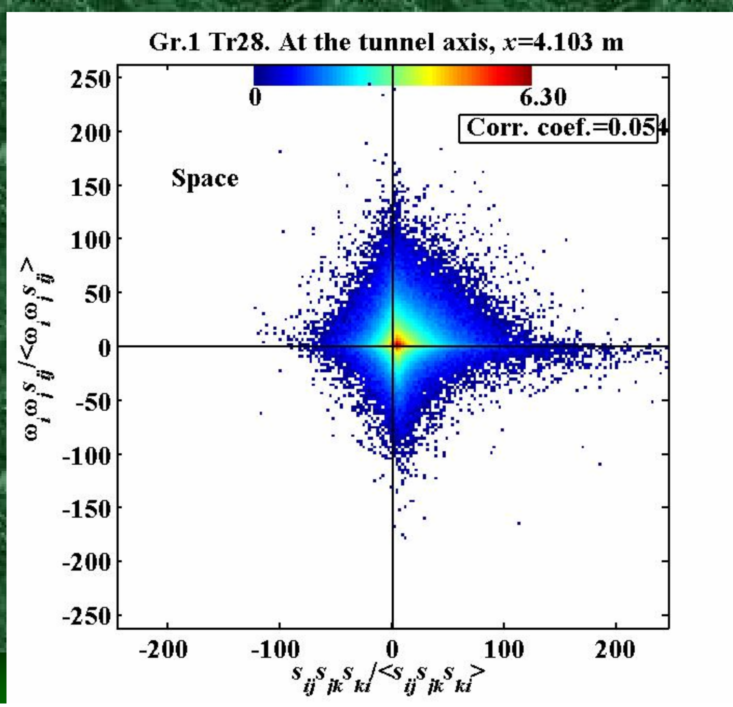
Gr.1 Tr28. At the tunnel axis, x=4.103 m
0
6.30
Corr. coef.=0.054
Space
$\omega_i\omega_j s_{ij}/\langle\omega_i\omega_j s_{ij}\rangle$
$s_{ij}s_{jk}s_{ki}/\langle s_{ij}s_{jk}s_{ki}\rangle$

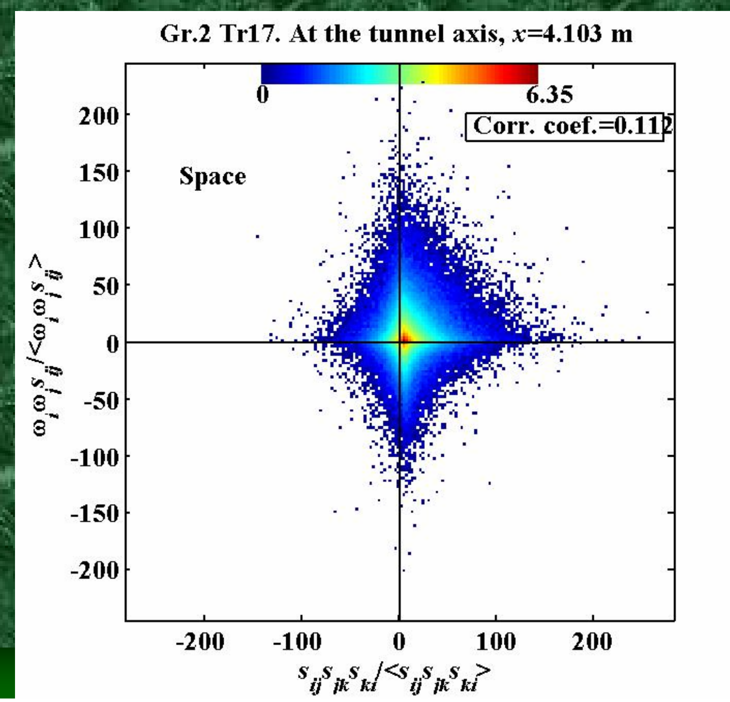
Gr.2 Tr17. At the tunnel axis, x=4.103 m
0
6.35
Corr. coef.=0.112
Space
$\omega_i\omega_j s_{ij}/\langle\omega_i\omega_j s_{ij}\rangle$
$s_{ij}s_{jk}s_{ki}/\langle s_{ij}s_{jk}s_{ki}\rangle$

R-Q PLOTS

More qualitative than others, e.g. the tails of the R-Q plots do not sit at the line where the discriminant D=0, which is not the case in 'normal ' mturbulence . It has to be seen whether this is a genuine flow property or is it mainly 'instrumental' or both

$$Q = \frac{1}{4}\left(\omega^2 - 2 s_{ik} s_{ik}\right)$$

$$R = -\frac{1}{3}\left(s_{ik} s_{km} s_{mi} + \frac{3}{4}\omega_i \omega_k s_{ik} \right)$$

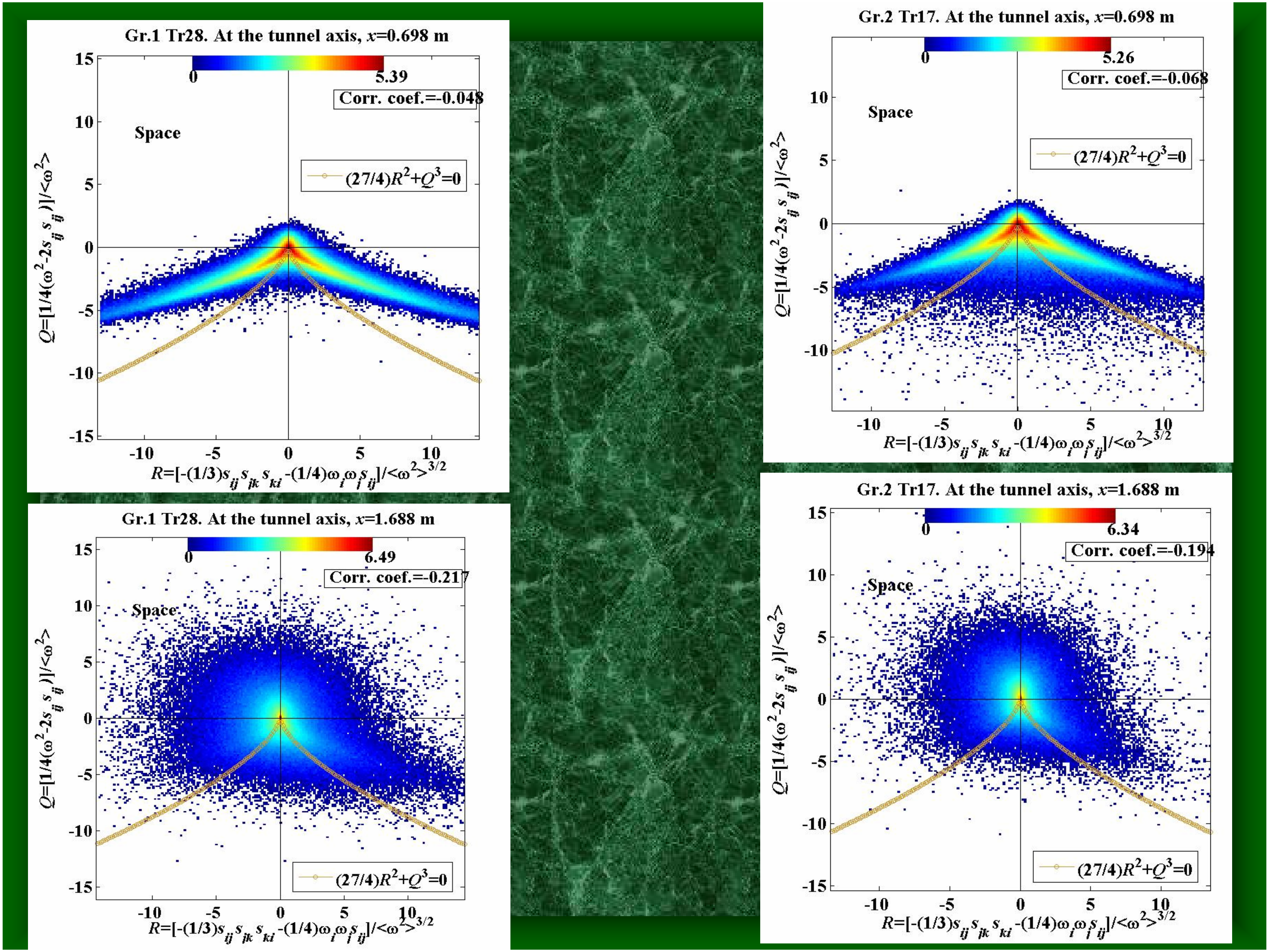

Gr.1 Tr28. At the tunnel axis, x=0.698 m
0
5.39
Corr. coef.=-0.048
Space
$(27/4)R^2+Q^3=0$
$Q=[1/4(\omega^2-2s_{ij}s_{ij})]/\langle\omega^2\rangle$
$R=[-(1/3)s_{ij}s_{jk}s_{ki}-(1/4)\omega_i\omega_j s_{ij}]/\langle\omega^2\rangle^{3/2}$
Gr.2 Tr17. At the tunnel axis, x=0.698 m
0
5.26
Corr. coef.=-0.068
Space
$(27/4)R^2+Q^3=0$
$Q=[1/4(\omega^2-2s_{ij}s_{ij})]/\langle\omega^2\rangle$
$R=[-(1/3)s_{ij}s_{jk}s_{ki}-(1/4)\omega_i\omega_j s_{ij}]/\langle\omega^2\rangle^{3/2}$
Gr.1 Tr28. At the tunnel axis, x=1.688 m
0
6.49
Corr. coef.=-0.217
Space
$(27/4)R^2+Q^3=0$
$Q=[1/4(\omega^2-2s_{ij}s_{ij})]/\langle\omega^2\rangle$
$R=[-(1/3)s_{ij}s_{jk}s_{ki}-(1/4)\omega_i\omega_j s_{ij}]/\langle\omega^2\rangle^{3/2}$
Gr.2 Tr17. At the tunnel axis, x=1.688 m
0
6.34
Corr. coef.=-0.194
Space
$(27/4)R^2+Q^3=0$
$Q=[1/4(\omega^2-2s_{ij}s_{ij})]/\langle\omega^2\rangle$
$R=[-(1/3)s_{ij}s_{jk}s_{ki}-(1/4)\omega_i\omega_j s_{ij}]/\langle\omega^2\rangle^{3/2}$

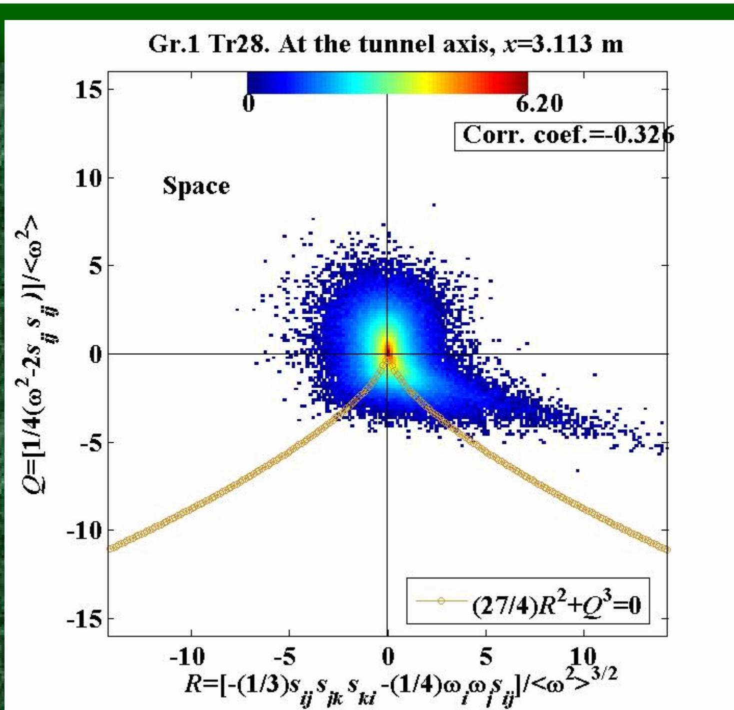
Gr.1 Tr28. At the tunnel axis, x=3.113 m
0
6.20
Corr. coef.=-0.326
Space
(27/4)R^2+Q^3=0
Q=[1/4(ω^2-2s_ij s_ij)]/<ω^2>
R=[-(1/3)s_ij s_jk s_ki -(1/4)ω_i ω_j s_ij]/<ω^2>^3/2

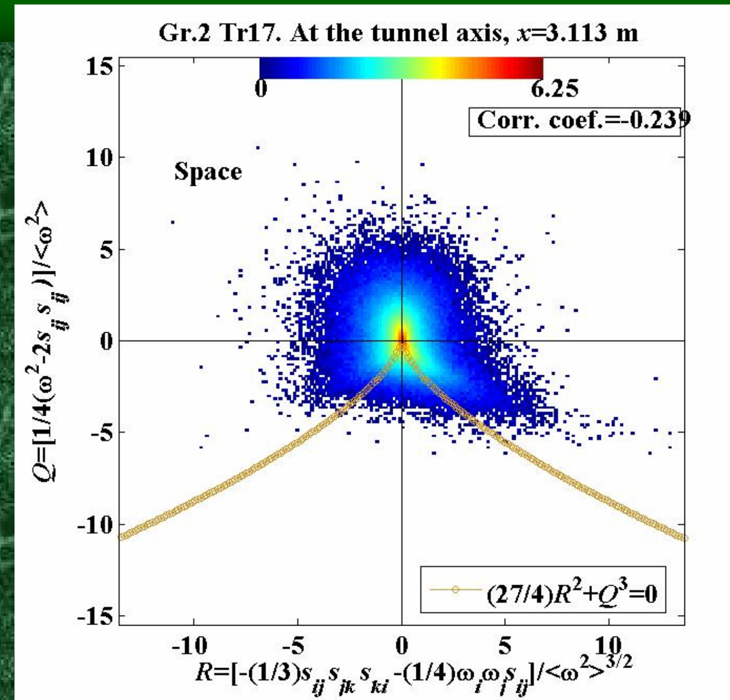
Gr.2 Tr17. At the tunnel axis, x=3.113 m
0
6.25
Corr. coef.=-0.239
Space
(27/4)R^2+Q^3=0
Q=[1/4(ω^2-2s_ij s_ij)]/<ω^2>
R=[-(1/3)s_ij s_jk s_ki -(1/4)ω_i ω_j s_ij]/<ω^2>^3/2

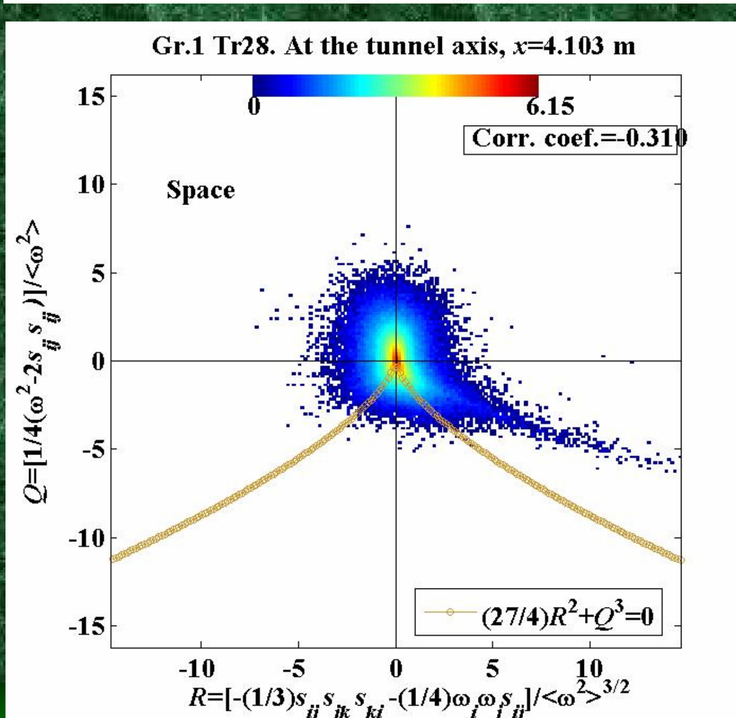
Gr.1 Tr28. At the tunnel axis, x=4.103 m
0
6.15
Corr. coef.=-0.310
Space
(27/4)R^2+Q^3=0
Q=[1/4(ω^2-2s_ij s_ij)]/<ω^2>
R=[-(1/3)s_ij s_jk s_ki -(1/4)ω_i ω_j s_ij]/<ω^2>^3/2

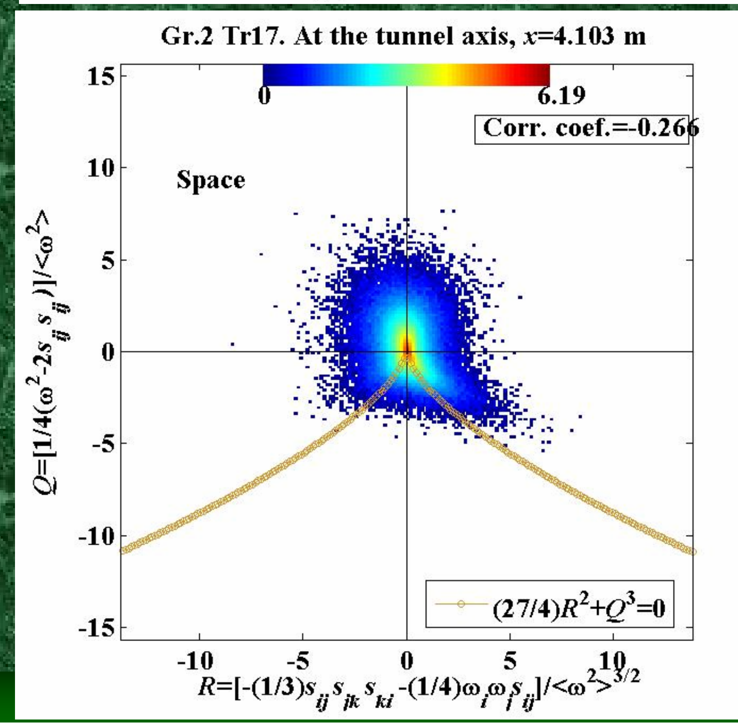
Gr.2 Tr17. At the tunnel axis, x=4.103 m
0
6.19
Corr. coef.=-0.266
Space
(27/4)R^2+Q^3=0
Q=[1/4(ω^2-2s_ij s_ij)]/<ω^2>
R=[-(1/3)s_ij s_jk s_ki -(1/4)ω_i ω_j s_ij]/<ω^2>^3/2

IN LIEU OF CONCLUSIONS

As mentioned at the very beginning the presented results are mostly of qualitative nature. Here we bring some preliminary conclusions which can be considered as “safe” along with some “less safe” considerations.

Among the motivations for the described experiments was the existence of a significant finite region of kinetic energy buildup reported first by HURST & VASSILICOS 2007 (HV) as exhibited among other things by existence of x_{peak} as is seen from slides 14 and 15. The latter exhibits significant TKE production at all flow accessible locations which is mainly due to streamwise gradients. HURST HURST VASSILICOS 2007 VASSILICOS 2007 and SEOUD & VASSILICOS 2007 (SV) do not quite observe this.

The Taylor microcsale as estimated using also full energy dissipation and enstrophy exhibits a tendency to become constant with distance as observed by HV and SV.
The energy dissipation rate appears to be smaller that in regular grids as exhibited in lower values of $C_\varepsilon \sim 0.1$ - 0.25 again in agreement with observations by SV. However, our results may be underestimated due to the underresolution of small scales (the probe is too large).
The streamwise velocity derivative skewness is pretty close to the conventional value 0.5, whereas it flatness is between 4 and 5 which is a somewhat smaller then observed in flows past regular grids at the same Re_λ. There seems to be an issue regarding the choice of Re_λ as a parameter for comparison: as pointed by SV the relation between Re_λ and Re is qualitatively different for fractal grids.

The statistics of the eigenvalues of the rate of strain tensor is very similar to that observed in ordinary turbulent flows.

The alignments between vorticity and the vortex stretching vector is similar to the "usual" at two two farther locations, but close to Gaussian at the two closest locations. This should be contrasted to the alignments between vorticity and the eigenframe of the rate of strain tensor which are essentially the same at all locations as in "usual" turbulent flows, i.e. the flow field is everywhere non-Gaussian. It has to be mentioned that at these locations the flow is far from being similar to "regular" turbulent flow and has distinct low frequency peaks.

The PDFs of enstrophy and strain production is qualitatively similar to that observed in ordinary turbulent flows at the three farthest locations, but are less skewed. At the closest location both are practically symmetric, and the PDFs of the strain production have much larger tails. These observations indicate that close to the grid the flow has reduced nonlinearity and is dominated by irrotational disturbances.

The PDFs of the components of velocity gradient tensor are qualitatively similar to that observed in ordinary turbulent flows, but the diagonal components are less skewed (the off diagonal are symmetric).

More qualitative than others are the R-Q plots, e.g. the tails of the R-Q plots do not sit at the line where the discriminant D=0, which is not the case in 'normal ' turbulence . It has to be seen whether this is a genuine flow property or is it mainly 'instrumental' or both.

Summarizing both a number of important differences along with several similarities with 'ordinary' grid flow were observed. ***Again we remind that the presented results and conclusions are preliminary and mainly qualitative - the quantitative aspects, e.g. numbers, require additional processing and checking.*** ***One of the key issues is the Reynolds number dependence. More conclusions to come after more work done on checks, additional processing (which includes the off center line data and a number of additional quantities) and related.***

MEANWHILE SOME QUESTIONS OF CONCEPTUAL NATURE

(There are much more)

MEMORY

What is the mechanism that turbulence does remember what happened (say, ‘locked in one scale’) at the inflow position and after undergoing some ‘adventures’ in the production region at $x < x_p$?

Why the flow does not remember, e.g. the strong inhomogeneity at the inflow position and in the production region?

STABILITY

Same as above – how/why this state (i.e. the one beyond x_{peak} claimed to be homogeneous and isotropic and ‘locked in one scale’) remains stable, i.e. why the flows does not want to turn into ‘normal’ turbulence?